Molecular, metabolic, and therapeutic aspects of respiratory complex III deficiency: *Bcs1l* mutant mice as an experimental model

Janne Purhonen

Folkhälsan Research Center

and

Stem Cells and Metabolism Research Program,
and Doctoral Program in Biomedicine,
Faculty of Medicine, University of Helsinki

Doctoral dissertation

To be presented for public discussion with the permission of
the Faculty of Medicine of the University of Helsinki,
in Lecture Hall 3, Biomedicum 1, Helsinki,
on the 16th of October, 2020, at 12 noon.

Supervisors:

Professor Vineta Fellman, MD, PhD
Folkhälsan Research Center, Helsinki, Finland
Children's Hospital, Helsinki University Hospital, Finland
Clinical Sciences Lund, Pediatrics, Lund University, Sweden
Stem Cells and Metabolism Research Program, Faculty of Medicine, University of Helsinki, Finland

Docent Jukka Kallijärvi, PhD
Folkhälsan Research Center, Helsinki, Finland
Stem Cells and Metabolism Research Program, Faculty of Medicine, University of Helsinki, Finland

Thesis committee:

Professor Vesa Olkkonen, PhD
Minerva Foundation Institute for Medical Research, Helsinki, Finland
Faculty of Medicine, University of Helsinki, Finland

Docent Risto Lapatto, MD, PhD
Faculty of Medicine, University of Helsinki, Finland
Children's Hospital, Helsinki University Hospital, Finland

Reviewers

Docent Eric Dufour, PhD
Faculty of Medicine and Health Technology, Tampere University, Finland

Doctor Christopher Carroll, PhD
Molecular and Clinical Sciences Research Institute, St. George's, University of London, UK

Opponent

Professor Michael Murphy, PhD
MRC Mitochondrial Biology Unit**,** University of Cambridge, UK

ISBN 978-951-51-6542-8 (paperback)
ISBN 978-951-51-6543-5 (PDF)
https://ethesis.helsinki.fi/

Unigrafia Oy
Helsinki 2020

TABLE OF CONTENTS

1 LIST OF PUBLICATIONS

Publications discussed in this thesis

I. **Purhonen J**, Rajendran J, Uusi-Rauva K, Katayama S, Krjutskov K, Einarsdottir E, Velapugi V, Kere J, Jauhiainen M, Fellman V, Kallijärvi J. Ketogenic diet attenuates hepatopathy in mouse model of respiratory chain complex III deficiency caused by a *Bcs1l* mutation. Sci Rep 2017; 7:957

II. **Purhonen J**, Rajendran J, Tegelberg S, Smolander O-P, Pirinen E, Kallijärvi J, Fellman V. NAD^+ repletion produces no therapeutic effect in mice with respiratory chain complex III deficiency and chronic energy deprivation. FASEB J 2018; 32: 5913-5926

III. Rajendran J, **Purhonen J**, Tegelberg S, Smolander OP, Mörgelin M, Rozman J, Gailus-Durner J, Fuchs H, Hrabe de Angelis M, Auvinen P, Mervaala E, Jacobs HT, Szibor M, Fellman V, Kallijärvi J. Alternative oxidase-mediated respiration prevents lethal mitochondrial cardiomyopathy. EMBO Mol Med 2019;11:e9456.

IV. **Purhonen J**, Grigorjev V, Ekiert R, Aho N, Rajendran J, Wikström M, Sharma V, Osyczka A, Fellman V, Kallijärvi J. A spontaneous mitonuclear epistasis converging on Rieske Fe-S protein exacerbates complex III deficiency in mice Nat Commun 2020;11:1–12.

In the text, these publications are referred to by their roman numerals (**I**-**IV**). In addition, relevant unpublished results are presented. Studies **I**, and **III**, have been previously included in the thesis of Jayasimman Rajendran (2019). The publications **I**, **III** and **IV** were reprinted under the Creative Commons CC BY licence. The publication **II** was reprinted with the permission from John Wiley & Sons, Inc.

Author's contribution

I, I wrote the manuscript draft and prepared all the images and tables. I took part in the design of the experiments. I conducted most of the laboratory analyses and analyzed the data: histology (Sirius Red, Oil-Red-O), interpretation and quantification of histological findings (excluding electron microscopy), enzyme activity measurements, protein analyses (SDS-PAGE, Blue-Native PAGE, and Western Blot), mtDNA copy number, qPCR, differential gene expression analysis and pathway analyses for transcriptomics data, statistics.

II, I wrote the manuscript draft and prepared all the images and tables. I took part in the study design. I conducted most of the laboratory analyses and analyzed the data: histology (Sirius Red, DAB-enhanced Prussian Blue), interpretation and quantification of histological findings, enzyme activity measurements, mitochondrial respirometry, protein analyses (SDS-PAGE and Western Blot), analysis of mitochondrial proteomics data (excluding raw data processing), statistics.

III, This study was the main thesis project of Jayasimman Rajendran. I contributed to the design of the experiments. I revised the manuscript. I set up and optimized several of the key methods for this study including isolation of mitochondria, mitochondrial respirometry, measurement of mitochondrial H_2O_2 emission and respiratory enzyme activities, measurement of protein carbonylation, and blue-native PAGE. I performed several of the assays myself or together with Jayasimman Rajendran. I prepared tools for the management and analysis of transcriptomics data (excluding raw data processing). I took part in the analysis and interpretation of transcriptomics data.

IV, I prepared all the manuscript figure panels, and most of the individual images and tables, and significantly contributed to writing and revising the manuscript text. I conducted most of the laboratory analyses on mouse samples and analyzed the data: sample collection, analysis and quantification of tissue histology, qPCR, ATP measurements, isolation of mitochondria, respirometry, measurement of respiratory enzyme activities, blue-native PAGE/Western blot, measurement of mitochondrial H_2O_2 emission, analysis of indirect calorimetry data, statistics.

2 ABBREVIATIONS

OXPHOS, oxidative phosphorylation
CIII, respiratory complex III (cytochrome bc_1 complex)
RISP, Rieske iron-sulfur protein (UQCRFS1)
NAD^+, Nicotinamide adenine dinucleotide, oxidized
AOX, alternative oxidase
NR, nicotinamide riboside
mtDNA, mitochondrial DNA
TCA cycle, tricarboxylic acid cycle (Kreb's cycle)
ATP, adenosine triphosphate
NADH, Nicotinamide adenine dinucleotide, reduced
GTP, Guanosine triphosphate
FADH, flavin adenine dinucleotide, reduced
CI, complex I
CII, complex II
CIV, complex IV
ETFDH, electron-transferring flavoprotein dehydrogenase
ETF, electron-transferring flavoprotein
ACAD, acyl-CoA dehydrogenase
DHODH, dihydroorotate dehydrogenase
SQOR, sulfide:quinone oxidoreductase
PRODH, proline dehydrogenase
CHDH, choline dehydrogenase
GPD2, glycerol 3-phosphate dehydrogenase
redox, reduction-oxidation
Q_o, quinol oxidation site
Q_i, quinone reduction site
heme b_L, low-potential heme *b*
heme b_H, high-potential heme *b*
AAA, ATPases associated with diverse cellular activities
ROS, reactive oxygen species
LHON, Leber Hereditary Optic Neuropathy
AMPK, AMP-activated protein kinase
SIRT1, sirtuin 1
PPARα, peroxisome proliferator-activated receptor alpha
PGC-1α, peroxisome proliferator-activated receptor gamma coactivator 1-alpha
AICAR, 5-aminoimidazole-4-carboxamide ribonucleotide
MELAS, mitochondrial encephalomyopathy, lactic acidosis, and stroke-like episodes
NADPH, nicotinamide adenine dinucleotide phosphate, reduced
NAMPT, nicotinamide phosphoribosyltransferase
NMN, nicotinamide mononucleotide
NRH, dihydro-nicotinamide riboside
E%, % of energy
P, postnatal day
NAAD, nicotinic acid adenine dinucleotide
FDR, false-discovery rate
ACLY, ATP citrate lyase
EPR, electron paramagnetic resonance

3 ABSTRACT

Mitochondrial disorders are rare diseases but collectively the most frequent group of inborn errors of metabolism. These disorders are genetically and phenotypically heterogenous and can manifest in any organ of the body with onset at any age. Mitochondrial functions are also diverse with the ATP production via the oxidative phosphorylation (OXPHOS) being the most notable. At the center of the OXPHOS machinery is the respiratory complex III (CIII, cytochrome bc_1 complex). CIII deficiency in GRACILE syndrome belonging to the Finnish disease heritage causes a neonatal-lethal hepatorenal disease. The primary cause of GRACILE syndrome is a c.A232G (p.S78G) mutation in the *BCS1L* gene, which encodes a translocase required for Rieske Fe-S protein (RISP, UQCRFS1) incorporation into CIII. Homozygous *Bcs1l*$^{p.S78G}$ mice bearing the GRACILE syndrome mutation recapitulate the human syndrome, but unlike the patients they have a short asymptomatic period and relatively longer lifespan giving a window for therapeutic interventions. In this thesis project, we studied two potential therapies aiming to improve dysfunctional mitochondria in *Bcs1l*$^{p.S78G}$ mice: ketogenic diet and NAD^+ repletion. We also utilized an alternative oxidase (AOX) transgene to bypass the electron-transfer blockade at CIII.

Ketogenic diets are low-carbohydrate high-fat diets causing nutritional ketosis. They have been proposed to induce a beneficial starvation-like adaptive mitochondrial response involving increased mitochondrial biogenesis. *Bcs1l*$^{p.S78G}$ mice tolerated the carbohydrate restriction of ketogenic diet, were able to utilize dietary fat as the main energy source and developed ketosis. Ketogenic diet attenuated the hepatic CIII assembly defect, increased CIII activity and corrected mitochondrial structural aberrations. Our results suggested that these changes were not due to increased mitochondrial biogenesis. In line with the improved CIII function, *Bcs1l* mutant mice showed attenuated hepatopathy as shown by delayed liver fibrosis, inhibited stellate cell activation and hepatic progenitor cell response, decreased cell death and plasma liver enzyme activities. Liver transcriptomics and subsequent histochemical analyses suggested altered macrophage activation and a normalizing effect by ketogenic diet.

In the second study, we characterized NAD^+ metabolism in *Bcs1l*$^{p.S78G}$ mice. We found transcriptionally repressed NAD^+ *de novo* biosynthesis and decreased hepatic NAD^+ concentration. Changes in NAD^+ consuming processes did not explain the decreased NAD^+ levels. Aiming to replete the NAD^+ levels, we fed the *Bcs1l*$^{p.S78G}$ mice a NAD^+ precursor nicotinamide riboside (NR). In contrast to previous studies on mitochondrial myopathy models and mouse models with secondary mitochondrial dysfunctions, the hepatic NAD^+ depletion of *Bcs1l*$^{p.S78G}$ mice was refractory to NR supplementation and the disease progression was unaltered. Cellular NAD^+ levels regulate mitochondrial functions via sirtuin deacetylases, which are the main targets of NAD^+ repletion therapies. Investigation of the upstream effectors of sirtuins showed that a starvation-like metabolic state of *Bcs1l*$^{p.S78G}$ mice is linked to AMP kinase and cAMP signaling, which likely counterbalances the repressive effect of decreased NAD^+ levels on the activity of SIRT1 and SIRT3.

In the third study, we introduced *Ciona intestinalis* AOX transgene into the *Bcs1l*$^{p.S78G}$ mice.

AOXs are non-mammalian enzymes that can bypass a blockade of the CIII-CIV segment of the respiratory electron transfer. The AOX-expressing *Bcs1l*$^{p.S78G}$ mice were viable, and their CIII-deficiency stimulated AOX-mediated respiration in isolated mitochondria. AOX expression tripled the median lifespan of *Bcs1l*$^{p.S78G}$ mice from 200 to 600 days. The extension of the lifespan was predominantly due to the complete prevention of late-onset cardiomyopathy. The effects of AOX were tissue specific. In the heart of *Bcs1l*$^{p.S78G}$ mice, it preserved normal tissue structure and function, mitochondrial morphology, respiratory electron transfer, and wild-type-like transcriptome. In contrast, AOX only minimally affected the late-stage liver disease. Whereas, in the kidneys, AOX normalized an atrophic kidney phenotype and some histological lesions but it did not normalize kidney function or cause global normalization of transcriptome changes. Our results suggest tissue-specific thresholds of CIII deficiency for *in vivo* AOX-mediated respiration in CIII deficiency. Moreover, our study demonstrates the value of AOX as a research tool to dissect the pathogenesis of CIII deficiency.

During our investigations, we observed approximately 5-fold difference in the lifespan of the *Bcs1l*$^{p.S78G}$ mice on two closely related congenic backgrounds. In the fourth study, we tracked the difference to a spontaneous homoplasmic mitochondrial DNA (mtDNA) variant (*mt-Cyb*$^{p.D254N}$) in an isolated congenic Lund University mouse colony. The variant changes a highly conserved negative amino acid residue in the only mtDNA-encoded subunit of CIII, cytochrome *b* (MT-CYB). A crossbreeding experiment utilizing the maternal inheritance of mtDNA verified the novel variant as the determinant of the survival difference. Functional studies showed that the variant exacerbated complex III deficiency in all assessed tissues. In otherwise wild-type mice, it also decreased cardiac CIII activity, caused a slight disturbance in mitochondrial bioenergetics, and decreased whole-body energy expenditure. Molecular dynamics simulations and their verification in isolated mutagenized *Rhodobacter capsulatus* cytochrome bc_1 complex showed that the *mt-Cyb*$^{p.D254N}$ variant restricts the mobility of RISP head domain movement.

In summary, these studies provided novel mechanistic and therapeutic insights into CIII deficiency at genetic, molecular, and metabolic level. The results highlight the importance of knowing the underlying tissue-specific pathology and metabolic adaptations when designing therapies for mitochondrial diseases. The genetic epistasis between *Bcs1l*$^{p.S78G}$ and *mt-Cyb*$^{p.D254N}$ also highlights the role of mitochondrial DNA background as a modifier of mitochondrial disease phenotypes.

4 TIIVISTELMÄ

Mitokondriotaudit ovat harvinaissairauksia, jotka kuitenkin ryhmänä muodostavat yleisimmän synnynnäisten aineenvaihduntahäiriöiden joukon. Mitokondriotautien mutaatioiden ja oireiden kirjo on erittäin laaja. Mitokondriotauti voi ilmetä lähes missä elimessä ja missä iässä tahansa. Mitokondriot ovat soluelimiä, joilla on lukuisia välttämättömiä tehtäviä. Näistä tunnetuin on ATP:n tuotanto oksidatiivisen fosforylaation avulla. Yksi keskeisistä entsyymeistä oksidatiivisessa fosforylaatiossa on hengitysketjun kompleksi III (sytokromi bc_1 -kompleksi). Suomalaiseen tautiperintöön kuuluvassa GRACILE-oireyhtymässä kompleksi III:n puutos aiheuttaa vastasyntyneiden kuolemaan johtavan maksa- ja munuaistaudin. Oireyhtymän aiheuttaa homotsygoottinen *c.A232G*-pistemutaatio (proteiinissa Ser78Gly) *BCS1L*-geenissä. BCS1L-proteiini on välttämätön Rieske rauta-rikki -proteiinin (RISP, UQCRFS1) kuljetukselle kompleksi III:een. Myös geneettisesti muokatuilla hiirillä homotsygoottinen *Bcs1l*$^{p.S78G}$ mutaatio aiheuttaa GRACILE-oireyhtymän kaltaisen taudin. Potilaisten poiketen mutanttihiirillä on lyhyt syntymän jälkeinen oireeton jakso ennen taudin puhkeamista, mikä mahdollistaa hoitokokeiden aloittamisen jo ennen taudin puhkeamista. Tämän väitöskirjan tutkimuksissa tutkimme kahta mahdollista hoitoa mitokondrioiden toiminnan kohentamiseksi GRACILE-oireyhtymän hiirimallissa: ketogeenistä ruokavaliota ja solujen NAD^+-määrän (nikotiiniamidiadeniinidinukelotidi) lisäämistä. Tutkimme myös kompleksi III:n puutoksen ohittamista vaihtoehtoista oksidaasia (AOX, *alternative oxidase*) ilmentävän siirtogeenin avulla.

Ketogeeniset ruokavaliot sisältävät erittäin niukasti hiilihydraatteja ja runsaasti rasvaa, mikä aiheuttaa ketoosin eli ketoaineiden lisääntymisen veressä. Ketogeenisen ruokavalion on esitetty käynnistävän osittaisen paastovasteen, johon liittyy mitokondrioiden toiminnan tehostuminen ja niiden lisääntynyt uudistuotanto. Koska *Bcs1l*$^{p.S78G}$-mutanttihiiret sopeutuivat ketogeeniseen ruokavalioon, ne ilmeisesti pystyivät hyödyntämään tehokkaasti rasvahappoja ja ketoaineita pääasiallisena energianlähteenä. Ketogeenisellä ruokavaliolla kompleksi III:een sitoutuneen RISP:n määrä lisääntyi mutanttihiiriillä, kuten myös kompleksi III:n aktiivisuus maksan mitokondrioissa. Nämä muutokset näkyivät myös maksan mitokondrioiden rakenteen normalisoitumisena. Tuloksemme viittasivat siihen, että mitokondrioiden toiminnan ja rakenteen parantuminen ei liittynyt lisääntyneeseen mitokondrioiden uudistuotantoon. Ketogeenisen ruokavalio hidasti merkittävästi maksataudin etenemistä, mikä näkyi muun muassa vähentyneenä stellaatti- ja ovaalisolujen aktivoitumisena, sekä vähentyneenä maksan sidekudostumisena. Myös maksaentsyymien aktiivisuudet plasmassa alenivat mutanttihiirillä. Maksan transkriptomiikka ja immunohistokemialliset värjäykset viittasivat siihen, että ketogeeninen ruokavalio vaikutti makrofagien toimintaan.

Väitöskirjan toisessa osatyössä tutkimme *Bcs1l*$^{p.S78G}$-hiirten NAD^+-aineenvaihduntaa. Havaitsimme, että mutanttihiirillä NAD^+-tuotannosta vastaavien geenien ilmentyminen oli vähentynyt kuten myös maksan NAD^+-pitoisuus. Muutokset NAD^+:tä kuluttavissa aineenvaihduntaprosesseissa eivät selittäneet NAD^+-pitoisuuden vähenemää. Syötimme *Bcs1l*$^{p.S78G}$-hiirille NAD^+:n esiastetta nikotiiniamidiribosidiä (NR) korjataksemme

puutoksen. Poiketen aiemmista tutkimuksista, joissa NR:llä on ollut parantava vaikutus mitokondriaalisten lihastautien hiirimalleissa, NR ei vaikuttanut *Bcs1l*$^{p.S78G}$-hiirten taudinkuvaan. NR ei myöskään vaikuttanut hoidon päätepisteessä mitattuun maksan NAD^+-pitoisuuteen. Solujen NAD^+-määrää kohentavien hoitojen yleinen tavoite on tehostaa NAD^+:sta riippuvaisten deasetylaasien, sirtuiinien, aktiivisuutta. Tutkimme sirtuiinien NAD^+:sta riippumattomia säätelymekanismeja ja havaitsimme, että mutanttihiirten nälkiintymistila aktivoi AMP-kinaasia ja cAMP-signalointia, jotka tunnetusti aktivoivat sirtuiini 1:tä ja 3:sta. Nämä muutokset oletettavasti kompensoivat vähentyneen NAD^+-määrän mahdollisia haitallisia vaikutuksia.

Kolmannessa osatyössä siirsimme *Ciona intestinalis* -vaippaeläimen AOX:ia koodaavan geenin *Bcs1l*$^{p.S78G}$-hiiriin. AOX:it ovat nisäkkäiltä puuttuvia mitokondrioiden entsyymejä, jotka voivat ohittaa soluhengityksen tukoksen kompleksi III:n tai IV:n kohdalla. AOX ei ollut haitallinen *Bcs1l*$^{p.S78G}$-hiirille ja kompleksi III:n toimintavajaus sai sen aktivoitumaan eristetyissä hiiren mitokondrioissa. *Bcs1l*$^{p.S78G}$-hiirille alkoi kehittyä 150 elinpäivän jälkeen sydänlihassairaus, mihin ne kuolivat keskimäärin 200 päivän iässä. AOX:ia ilmentäville mutanttihiirille ei kehittynyt lainkaan sydäntautia, ja niiden mediaanielinikä oli 600 päivää. AOX esti täysin sydäntautiin liittyvän sydämen laajentuman ja toiminnan heikkenemisen. Sydämen mitokondrioissa AOX korjasi soluhengityksen sekä mitokondrioiden rakenteen muutokset. Vastaava pelastavaa vaikutusta AOX:illa ei ollut maksatautiin 150-200 päivän ikäisillä *Bcs1l*$^{p.S78G}$-hiirillä. Munuaisissa taas AOX osittain korjasi tai esti kudosrakenteen muutoksia, mutta vaikutti vain vähäisesti tämän elimen toimintaan. Tuloksemme osoittivat, että AOX:n vaikutukset ovat kudoksesta riippuvaisia kompleksi III:n puutoksessa ja että se on hyödyllinen työkaluksi kompleksi III:n tautimekanismien tutkimuksessa.

Tutkimustemme alkuvaiheessa huomasimme noin viisinkertaisen eron *Bcs1l*$^{p.S78G}$-hiirten eliniässä kahden eri hiirikannan välillä. Väitöskirjan neljännessä osatyössä löysimme koko genomin sekvensoinnilla homoplasmiseen yhden nukleotidin muutokseen Lundin yliopiston hiirikannan mitokondrio-DNA:ssa. Muutos vaihtaa negatiivisesti varautuneen aspartaatin neutraaliin asparagiiniin (D254N) sytokromi b -proteiinissa (MT-CYB). MT-CYB on kompleksi III:n alayksiköistä ainoa, jonka geeni sijaitsee mitokondrio-DNA:ssa. Käyttäen hyväksi mitokondrio-DNA:n maternaalista periytymistä osoitimme *mt-Cyb*$^{p.D254N}$-variantin aiheuttavan *Bcs1l*$^{p.S78G}$-hiirten varhaisen kuoleman n. kuukauden iässä. Kuten oletimme *mt-Cyb*$^{p.D254N}$ pahensi *Bcs1l*$^{p.S78G}$-hiirten kompleksi III:n puutosta kaikissa tutkimissamme kudoksissa. Yksinäänkin *mt-Cyb*$^{p.D254N}$ vähensi sydämessä kompleksi III:n aktiivisuutta, aiheutti pienen häiriön hengitysketjun toiminnassa ja pienensi hiirten energiankulutusta. Kompleksi III:n rakenteen tietokonemallinnukset ja biofysikaaliset tutkimukset *Rhodobacter capsulatus* -bakteerin sytokromi bc_1-kompleksissa osoittivat, että D254N-aminohappomuutos häiritsee RISP:n elektroneja siirtävän domeenin liikettä kompleksi III:ssa.

Tämän väitöskirjan tutkimukset tuottivat uutta tietoa kompleksi III:n puutoksen tautimekanismeista ja mahdollisista hoidoista. Tuloksemme osoittavat, että on tärkeää tuntea mitokondriotaudin kudoskohtaisia ja vaihtelevia aineenvaihduntamuutoksia suunniteltaessa hoitoja. *Bcs1l*$^{p.S78G}$-mutaation ja *mt-Cyb*$^{p.D254N}$-variantin yhteisvaikutus puolestaan osoitti, että geneettinen tausta voi vaikuttaa odottamattomalla tavalla mitokondriotaudin kulkuun.

5 INTRODUCTION

An estimated two billion years ago, an engulfment of an ancient relative of α-proteobacterium by a host cell, putatively related to *Asgard archaea*, gave rise to the mitochondrion, a double membrane-enclosed organelle performing cellular respiration.[1,2] This event evolved into a vital endosymbiosis that defines all eukaryotes from protists, fungi, and plants to animals.[3] How the tricarboxylic acid cycle (TCA cycle, also known as Kreb's cycle) functions as a bioenergetic and biosynthetic hub, and how mitochondrial respiratory enzymes generate the electrochemical potential coupled to adenosine triphosphate (ATP) production were the seminal discoveries of the decades from 1930s to 1970s.[4–6] Research during the past two decades has recognized mitochondria as vital players in many areas of cell signaling and metabolism.[7] The identification of full human mitochondrial proteome is also essentially completed.[8] However, of the more than 1000 mitochondrial proteins many still lack functional annotation. Meanwhile, modern genetics has allowed more and more monogenic mitochondrial diseases to be identified.[9] Unfortunately, the treatments for mitochondrial diseases lack far behind the diagnostic capabilities, despite the fact that mitochondrial diseases are, as a group, the most common in-born errors of metabolism.[9,10] Many multigenic globally epidemic chronic diseases such as cancer, obesity, obesity-associated metabolic syndrome, Alzheimer's and Parkinson's diseases, have also an inherent link to mitochondria, the organelles that affect essentially all aspects of cellular metabolism.[11]

At the heart of virtually all energy-transducing respiratory electron-transfer systems in bacteria and in the mitochondria of eukaryotes lies the cytochrome bc_1 complex, also known as quinol-cytochrome c oxidoreductase and in the mitochondria as complex III (CIII).[12] CIII catalyzes the oxidation of the lipid electron carrier ubiquinol (reduced coenzyme Q) to ubiquinone (oxidized coenzyme Q) while passing on electrons to the soluble electron carrier cytochrome *c*, a substrate for the terminal oxidase cytochrome *c* oxidase (complex IV, CIV), which reduces oxygen to water. During the electron transfer, the respiratory complexes I, III and IV translocate protons to generate an electrochemical potential required for ATP synthesis. In mammalian mitochondria, CIII is vital for the availability of oxidized coenzyme Q and for the whole respiratory electron transfer.

CIII deficiencies are relatively rare mitochondrial diseases and most often caused by mutations in the *MT-CYB* and *BCS1L* genes.[13] *BCS1L* encodes a mitochondrial inner-membrane translocase required for the incorporation of the Rieske Fe-S protein (RISP, UQCRFS1) into CIII.[13,14] This process is compromised in GRACILE syndrome due to a c.A232G (p.S78G) mutation in *BCSL*.[15,16] GRACILE syndrome is a severe neonatal mitochondrial disease belonging to the Finnish disease heritage. The name of the syndrome derives from main clinical features: growth restriction, aminoaciduria, cholestasis, iron overload, lactic acidosis and early neonatal death.[15,17] To study the pathogenesis and potential treatments of GRACILE syndrome, Prof. Fellman's research group generated a patient mutation knock-in mouse model some ten years ago.[18] Similarly to the patients, the homozygous $Bcs1l^{p.S78G}$ mutation causes early-onset hepatorenal disease with growth restriction in mice. This thesis project set out to study dietary and pharmacological interventions, and xenogenic alternative oxidase-mediated bypass of CIII in the $Bcs1l^{p.S78G}$ mice. During the process, we identified and studied a novel mtDNA variant acting as a modifier of the CIII deficiency caused by the $Bcs1l^{p.S78G}$ mutation.

6 REVIEW OF LITERATURE

6.1 Mitochondria

6.1.1 Structure and function of mitochondria

Mitochondria are double-membraned cellular organelles the size, shape, and abundance of which vary widely between different tissues, cell types, and metabolic states (Fig. 1).[19,20] The outer membrane is permeable to most small molecules while the folded inner membrane, heavily packed with the respiratory complexes, forms an impermeable barrier separating the mitochondrial matrix from the mitochondrial inner-membrane space and cytoplasm. The folds of the inner membrane are called cristae. Their presumed function is to maximize the surface area of the membrane and locally condense the electrochemical potential to maximize the efficacy of ATP production. Mitochondrial morphology is highly dynamic and responds to metabolic demands such as those induced by feeding, fasting, and mitochondrial defects.[21] Furthermore, mitochondria are inter-connected organelles that form a mitochondrial network, and also physically interact with other organelles such as endoplasmic reticulum and lipid droplets. Mitochondrial fission and fusion events largely regulate the morphology of individual mitochondria but also the shape of the mitochondrial network.

Figure 1. An electron micrograph showing mitochondria (dark electron-dense structures) of different sizes and shapes in a renal proximal tubule cell. Several cristae (yellow arrowheads) can be observed in most of the mitochondria.

Mitochondria have their own small genome, and transcription, translation, and replication machineries.[22] In humans, the mitochondrial DNA (mtDNA) encodes 22 transfer RNAs, 2 ribosomal RNAs, and 13 vital structural and catalytic subunits of respiratory complexes and ATP synthase. The nuclear DNA encodes the rest, the vast majority, of the mitochondrial proteins which are translated by cytoplasmic ribosomes and then imported into mitochondria. In every mitochondrion there can be multiple copies of mtDNA and in every cell hundreds to thousands of copies.

6.1.2 Respiratory electron transfer and oxidative phosphorylation

Mitochondria are best known for their function as highly efficient producers of ATP, a high-energy compound that fuels cellular metabolism.[7] Anaerobic glycolysis produces 2 ATP molecules per glucose, whereas the full oxidation of glucose through cellular respiration produces approximately 32 ATPs. Mitochondria achieve this by the serial reactions of the TCA cycle that generate the reduced cofactors NADH, GTP and FADH.[7,23] Consequently, NADH and FADH serve as substrates for the respiratory electron transfer (Fig. 2). Complex I (CI), NADH dehydrogenase, oxidizes NADH to NAD^+ with a subsequent reduction of the lipid electron carrier ubiquinone to ubiquinol (oxidized and reduced coenzyme Q, respectively). The TCA cycle enzyme complex II (CII), succinate dehydrogenase, oxidizes succinate to fumarate while reducing the integrated cofactor FAD to FADH and consequent electron transfer from FADH to ubiquinone. The next enzyme in the electron transfer process is CIII, which accepts electrons from ubiquinol and passes them on to the soluble electron carrier, cytochrome *c*. The terminal oxidase in the mammalian mitochondria is complex IV (CIV, cytochrome *c* oxidase), which oxidizes cytochrome c and reduces oxygen to water, the very reaction seen as cellular respiration. Three of these respiratory enzymes contribute to the generation of the electrochemical potential by translocating protons from the matrix to the inter-membrane space, CI, CIII and CIV. The electrochemical potential comprises two factors: the electric difference (electric potential) and pH difference (chemical potential) across the membrane. The backflow of protons at ATP synthase catalyzes the conversion of ADP and inorganic phosphate to ATP. The respiratory electron transfer (cellular respiration) that is coupled to the phosphorylation of ADP is termed oxidative phosphorylation (OXPHOS).[24]

The initiation of respiratory electron transfer is not limited to CI and CII (Fig. 2). In many cells, several other mitochondrial inner-membrane enzymes also utilize ubiquinone or cytochrome c as an electron acceptor, and therefore contribute to OXPHOS. The electron-transferring flavoprotein dehydrogenase (ETFDH) serves as a hub for more than ten flavoproteins that transfer the electrons via the electron-transferring flavoprotein (ETF) to ETFDH, which then transfers the electrons to ubiquinone.[25,26] The most notable ETFDH-linked enzymes are acyl-CoA dehydrogenases (ACADs) of the fatty acid oxidation. Disruption of the respiratory electron transfer renders mammalian cells auxotrophic for uridine.[27,28] This is because the dihydroorotate dehydrogenase (DHODH) of uridine biosynthesis pathway requires ubiquinone as an electron acceptor. Other less

recognized respiratory enzymes include sulfide:quinone oxidoreductase (SQOR)[29], proline dehydrogenase (PRODH)[30], choline dehydrogenase (CHDH)[31], and glycerol 3-phosphate dehydrogenase (GPD2)[32]. Like DHODH, these also connect to cellular respiration at the level of ubiquinone. Moreover, a mitochondrial intermembrane space sulfhydryl oxidase GFER, involved in oxidative protein folding, and sulfite oxidase (SUOX) directly reduce cytochrome *c* bypassing the ubiquinone pool and CIII.[33,34]

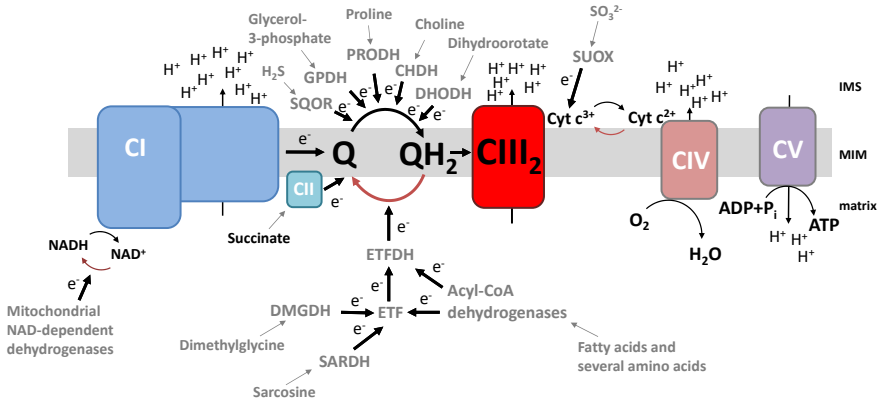

Figure 2. The mitochondrial respiratory electron transfer system. The arrows and e^- (electrons) mark the direction of reducing equivalents. Because of space limitations, some mitochondrial inner-membrane (MIM) enzymes (SQOR, GPDH, PRODH, CHDH, DHODH, and ETFDH) are placed outside the membrane. Abbreviations: Q, ubiquinone; QH_2, ubiquinol; Cyt c^{3+}, oxidized cytochrome c; Cyt c^{2+}, reduced cytochrome c; H^+ proton; IMS, inner-membrane space; MIM, mitochondrial inner membrane.

6.1.3 Role of mitochondria beyond bioenergetics

Mitochondria have many functions beyond the OXPHOS. The TCA cycle is not only needed to drive energy metabolism, but it is also an important source of precursors for many biosynthetic processes.[7,23] As an example, the TCA cycle intermediate citrate serves as a carbon source for de novo lipogenesis while succinyl-CoA for heme biosynthesis. Mitochondria are also important for reduction-oxidation (redox) balance and compartmentalization of reducing equivalents.[7,35] Without cellular respiration, glycolysis will lead to the accumulation of lactate and the reduced cofactor NADH. Some unicellular organisms can excrete lactate to environment, but in multicellular organisms prolonged whole-body anaerobic glycolysis leads to metabolic acidosis. Many vital biosynthetic processes occur partly in cytoplasm and partly in mitochondria. For instance, the mitochondrial enzyme ALAS1 initiates heme biosynthesis, but cytoplasmic enzymes catalyze the subsequent steps until the two finals steps that again take place in the mitochondria.[36] Some rare eukaryote species that have lost respiratory enzymes during evolution still have mitochondrial remnants harboring the enzymes required for the biosynthesis of iron-sulfur clusters.[37] For some metabolic processes, similar enzymes, yet encoded by different genes, exist in cytoplasm and mitochondria. As an example, folate

and methionine cycles operate in the cytoplasm and in the mitochondria with partial redundancy.[38]

Many important detoxification reactions also take place in mitochondria.[7] The mitochondrial enzymes carbamoyl phosphate synthetase and ornithine transcarbamoyl transferase link urea cycle to mitochondria. Urea cycle is a detoxification process, mainly in the liver and to some degree in the kidneys, whereby toxic ammonia from amino acid catabolism is converted to urea to be excreted via urine. Metabolism of sulfur-containing amino acids releases hydrogen sulfide, a highly toxic metabolite, which inhibits several heme proteins, including CIV.[7,29] The physiological amounts of hydrogen sulfide generated by cellular catabolism are, however, efficiently detoxified by the respiratory enzyme SQOR. Mitochondria have been noted as a major source of cellular hydrogen peroxide, but according to recent findings they may also serve as a sink for hydrogen peroxide.[39,40]

Mitochondria interact with the rest of the cell in various ways.[23,41] AMP-activated protein kinase (AMPK) senses insufficient OXPHOS capacity by monitoring cellular adenylate phosphorylation status to drive a suitable adaptive mitochondrial response.[42] The TCA cycle metabolites such as acetyl-CoA are important for protein posttranslational modifications.[23] The respiratory electron transfer leaks some electrons directly to oxygen which leads to the production of superoxide, an oxygen radical. Superoxide is rapidly converted to hydrogen peroxide by superoxide dismutases.[41] Superoxide and hydrogen peroxide were once thought to be only harmful byproducts of OXPHOS. However, nowadays hydrogen peroxide is recognized to be an important signaling molecule regulating for example angiogenesis and cellular differentiation.[41] Perhaps the most dramatic mitochondria-derived signal is the initiation of apoptosis by cytochrome *c* release.[43]

6.2 Respiratory complex III (CIII, cytochrome bc_1 complex)

6.2.1 The Q cycle

CIII, or more generally cytochrome bc_1 complex, is an evolutionarily ancient enzyme and its three catalytic subunits are highly conserved among bacteria and eukaryotes.[12] In its simplest form, such as in *Rhodobacter capsulatus*, cytochrome bc_1 complex contains only the key three catalytic subunits: RISP, cytochrome *b* and cytochrome c_1. Higher organisms have gained additional subunits around these three vital catalytic components during evolution. The mammalian CIII comprises eleven subunits.[13] The exact functions of the additional subunits remains largely unknown.

Cytochrome bc_1 complexes operate under the Q-cycle mechanism (Fig. 3).[12,44] The cycle initiates at the quinol oxidation site (Q_o) where the iron-sulfur cluster of RISP accepts the first electron from ubiquinol converting the ubiquinol to an unstable semiquinone. After this, the low potential heme *b* (heme b_L) of cytochrome *b* accepts the second electron from the semiquinone, generating ubiquinone. RISP transfers the first electron to cytochrome c_1, which then reduces the soluble electron carrier cytochrome *c*. The parallel electron transfer

through two heme centers of cytochrome *b* mediate the reduction of ubiquinone at the quinone reduction site (Q_i). During the Q cycle, cytochrome bc_1 both oxidizes ubiquinol to ubiquinone but also reduces ubiquinone to ubiquinol with the net reaction in the favor of ubiquinol oxidation. The steps of the Q cycle are coupled to the release of four protons into the mitochondrial inner-membrane space per ubiquinol oxidized.

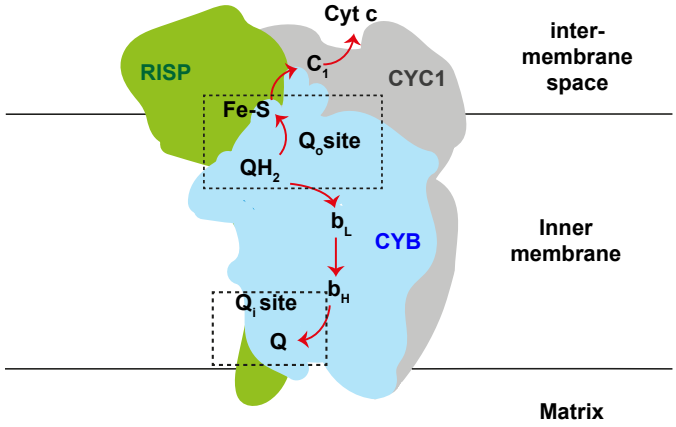

Figure 3. Operation of Q cycle in cytochrome bc_1 complexes. The three catalytic subunits are shown, and the flow of electrons are marked with red arrows. For clarity, only one monomer of the dimeric complex is shown. Abbreviations: RISP (UQCRSFS1), Rieske-iron sulfur protein; CYB, cytochrome *b*; CYC1, cytochrome c_1; Cyt c, cytochrome *c*; QH_2, quinol; Q, quinone; Q_o quinol oxidation site; Q_i, quinol reduction site; Fe-S, iron-sulfur cluster of RISP; b_L, low-potential heme *b* of CYB; b_H, high-potential heme *b* of CYB.

6.2.2 CIII structure and assembly, and the role of BCS1L

The mammalian CIII is a homodimer with each monomer thought to comprise eleven subunits.[45,46] However, according to a recent re-analysis of high-resolution crystal and cryo-electron microscopy structures, the eleventh subunit, a RISP N-terminal fragment, is shared between the monomers, making the dimer a 21-subunit entity.[46] mtDNA encodes only one of the CIII subunits, MT-CYB. Nuclear DNA encodes the rest of the complex. Yeast studies have delineated the steps of CIII assembly, and all evidence suggests that the process is highly similar in mammals.[13,47] The construction of CIII monomer starts from MT-CYB and its hemylation. At least three assembly factors (UQCC1, UQCC2 and UQCC3) take part in the initial steps of the process, most likely by stabilizing the pre-complex. The dimerization of CIII is an early event and follows soon after incorporation of the core proteins (UQCRC1 and UQCRC2).[47] The finals steps of CIII assembly are known in most detail and involve the insertion of the essential catalytic subunit RISP (Fig. 4A).[14] RISP is imported into mitochondria via the common TOM-TIM23 import system. In the matrix, RISP gains its iron-sulfur cluster with LYRM7 (Mzm1 in yeast) serving as a scaffold.[48] Then, BCS1L translocates the partially or even fully folded RISP back to the mitochondrial inner-membrane space followed by its insertion into CIII.[49]

BCS1L belongs to AAA family proteins (ATPases associated with diverse cellular activities) based on sequence similarity. BCS1L monomer has three domains: a transmembrane domain in the N-terminus followed by a unique BCS1L-specific domain, and ATPase domain similar to AAA-ATPases in the C-terminus (Fig. 4B).[14] Yeast Bcs1 contains an internal mitochondrial targeting sequence but the same segment is not conserved in mammals.[50] Recently, two groups independently determined the structure of yeast Bcs1[51] and mouse[52] BCS1L. Unlike other AAA-ATPases, which are typically hexamers and participate in protein unfolding and degradation,[53] BCS1L is a heptamer that translocates a folded substrate utilizing a specialized airlock-type translocation mechanism.[51,52] The uniqueness of BCS1L for the ability to translocate a partially of fully folded protein, while preserving mitochondrial inner membrane intactness and membrane potential, likely means that the RISP is its only substrate.

After insertion into the complex, RISP goes through a proteolytic cleavage of the N-terminus containing the mitochondrial targeting sequence.[54,55] The core proteins UQCRC1 and UQCRC2 which are homologous to matrix-processing peptidase likely perform the cleavage.[55,56] Intriguingly, one of the N-terminus fragments forms the eleventh subunit of CIII in mammals but not in yeast.[46,54] A study characterizing the CIII-interacting protein TTC19 suggests it plays a role in the clearance of the unneeded extra N-terminus fragments from RISP.[55]

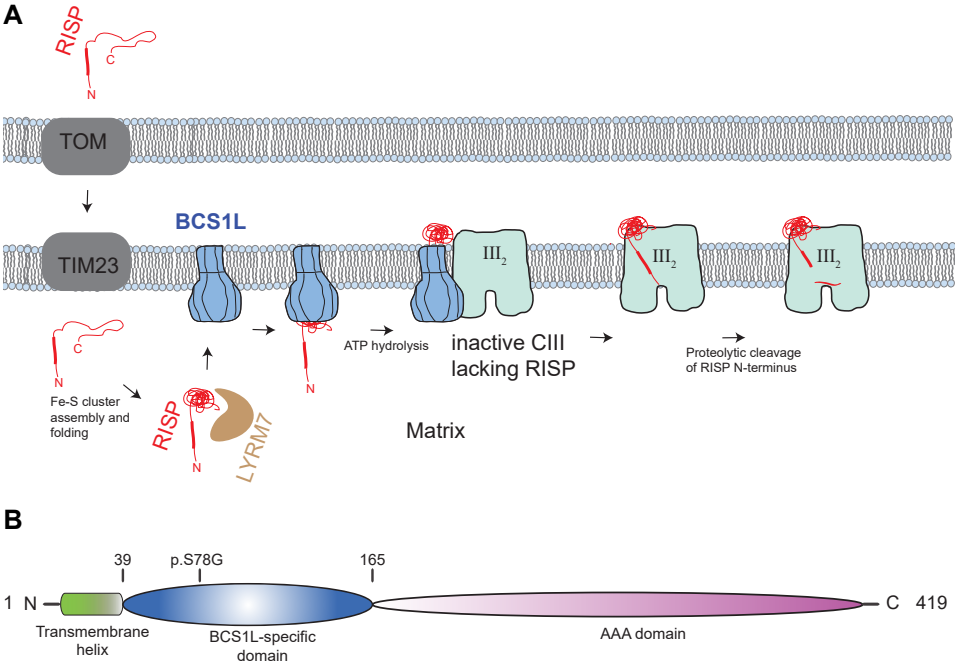

Figure 4. Role of BCS1L in RISP (UQCRFS1) assembly into CIII. (**A**) A schematic simplification of RISP mitochondrial import, assembly into CIII, and processing. (**B**) Three domains of human BCS1L. GRACILE syndrome mutation is located at amino acid residue 78 (p.S78G). AAA, ATPases associated with various cellular activities.

A large proportion of CIII dimers physically connect to CI and or CIV to form large structural entities called supercomplexes.[57,58] The composition and stoichiometry of supercomplexes vary in a cell type-specific manner. In addition, new evidence suggests the existence of supercomplexes in which mitochondrial fatty acid oxidation enzymes trifunctional protein and ETFDH physically interact with CI and CIII, respectively.[59] The physiological significance of supercomplexes is under debate.[57,58] The supercomplexes may compartmentalize the coenzyme Q and cytochrome *c* between their respective reaction centers with a kinetic advantage and attenuation of harmful side reactions leading to superoxide production. However, almost an equal amount of evidence for and against this theory exits.[58] It remains possible that the supercomplex formation is solely an inevitable consequence of the high protein density in the inner mitochondrial membrane and a solution to prevent protein aggregation.

6.2.3 Superoxide production by CIII

CIII is one of the mitochondrial sources of superoxide, an oxygen radical and a precursor for other reactive oxygen species (ROS).[60] CIII can uniquely emit superoxide to both sides of the mitochondrial inner membrane: into matrix and inner-membrane space. The superoxide in the inner-membrane space enzymatically or spontaneously dismutates to hydrogen peroxide, which can take part in cellular signaling as it can reach the cytoplasm. The superoxide production takes place at the Q_o site and derives from the unstable semiquinone intermediate.[61] Mutations and inhibitors that affect the catalytic function of CIII may either increase or decrease the superoxide production.[62] Typically, inhibitors (e.g. antimycin A) or mutations that block the Q_i site enhance the superoxide production. In contrast, inhibitors (e.g. stigmatellin or myxothiazol) or mutations that inhibit the quinol oxidation decrease or completely block the superoxide production. Mitochondrial membrane potential has also a profound effect on the superoxide production by CIII.[63] In fact, isolated native CIII or other cytochrome bc_1 complexes do not produce a measurable amount of superoxide in the absence of membrane potential unless the enzyme is inhibited by antimycin A.[63,64] CIII is also an important determinant of superoxide production elsewhere in the respiratory electron transfer, as it modulates the redox status of the coenzyme Q pool. Over-reduced coenzyme Q pool may lead to reverse-electron flow reactions, most notably at the level of CI.[65]

6.3 Mitochondrial diseases

Mitochondrial diseases are a clinically and genetically diverse group of in-born errors of metabolism caused by mutations in nuclear DNA and mtDNA.[9] Their estimated collective prevalence is one per 5000 births.[10] A mitochondrial disease may present as myopathy, cardiomyopathy, hepatopathy, kidney disease, neurological disorder, endocrine and hematological disturbance, or with other symptoms in isolation or in various combinations with onset at any age.[9] The inheritance of mitochondrial diseases caused by nuclear DNA

mutations follows the Mendelian rules. In contrast, mtDNA is maternally inherited. Because mtDNA is a multicopy genome, mtDNA mutations can be homoplasmic or heteroplasmic. In heteroplasmy, both wild-type and mutated mtDNA exist in different proportions. The degree of heteroplasmy may vary between different tissues and cell types. The inheritance of mtDNA mutation load is unpredictable due to a bottle-neck phenomenon in mtDNA amount during female germline development.[66]

6.3.1 CIII deficiencies

CIII deficiencies are relatively rare mitochondrial diseases.[13] Over 40 mutations have been found in *MT-CYB* and over 20 mutations in *BCS1L*. Mutations in other CIII-related genes, mainly encoding auxiliary subunits (*UQCRB*[67], *UQRCQ*[68] and *UQCRC2*[69]) or assembly factors (*LYRM7*[70], *UQCC2*[71], *UQCC3*[72], *TTC19*[73]), are limited to a few cases. Excluding the patients with mutations in MT-CYB, only four patients have been reported with mutations in the two other catalytic subunits: in RISP[74] and in cytochrome c_1 (*CYC1*)[75]. Symptoms in CIII deficiencies are diverse, as typical of mitochondrial diseases, and range from exercise intolerance[76] to severe neurological manifestations[68], and early-onset lethal metabolic crises[15]. Even mutations in the same gene and affecting the same part of the protein can cause vastly different phenotypes.[77]

6.3.2 MT-CYB mutations and polymorphisms

The MT-CYB protein has its highly conserved regions preserved in bacteria, plants, and animals but, overall, it is also highly polymorphic.[13] In fact, forensic researchers commonly utilize the *MT-CYB* nucleotide sequence for species identification.[78] In humans, more than 450 missense changes exist in *MT-CYB* according to the Human Mitochondrial Genome Database (mitomap.org[79]). Not surprisingly, *MT-CYB* mutations were the first identified causes of CIII deficiency.[76,80,81] The majority of the identified *MT-CYB* mutations are sporadic and heteroplasmic, with typically high mutation load in skeletal muscle.[13] Frequently, *MT-CYB* mutations manifest as exercise intolerance and progressive myopathy,[13,76] sometimes as cardiomyopathy[82]. In contrast to nuclear mutations affecting CIII, which typically manifest soon after birth, *MT-CYB* mutation-related pathology commonly emerges at childhood or adulthood.[13] In some patients, central nervous system manifestations accompany the myopathic features.[83–85] Only one verified case of CIII deficiency has been homoplasmic for a *MT-CYB* mutation.[86] This mutation led to a neonatal-lethal multisystemic disease. In addition, *MT-CYB* mutations and variants appear to contribute to Leber Hereditary Optic Neuropathy (LHON) caused by mutations in mtDNA-encoded CI subunits.[13] A homoplasmic *MT-CYB* variant has also presumably exacerbated a CIII deficiency with unidentified nuclear origin.[87]

The characterization of *MT-CYB* mutations have proven challenging due to the lack of technology to introduce targeted mutations into the mammalian mtDNA. Therefore,

biochemical studies have relied on yeast[88] and bacterial models[89], where *MT-CYB* homologs are amenable to genetic manipulation, or transmitochondrial cybrid cells[87]. Interestingly, some non-pathogenic human *MT-CYB* variants studied in yeast have shown a rather profound effect on CIII function despite the non-pathogenic nature.[90] Moreover, some *MT-CYB* variants possibly alter pharmacological responses to drugs with affinity for Q_o site of CIII such as the anti-malarial drug atovaquone and the antidepressant clomipramine.[90]

6.3.3 BCS1L mutations and GRACILE syndrome

BCS1L mutations are the most common diagnosed cause of CIII deficiency.[91] All identified *BCS1L* mutations are recessive and spread across the three domains of the protein with no clear genotype-phenotype correlation (Fig.4B).[77] However, the recently published crystal and cryo-electron microscopy structures of BCS1L may bring new insights into the phenotypic variability among the *BCS1L* mutations.[51,52] The symptoms in BCS1L-related pathologies range from Björnstad syndrome[77] with sensorineuronal hearing loss and aberrant hair phenotype to lethal metabolic crises of neonates.[91] A common onset is at fetal period or soon after birth. Excluding the Björnstad syndrome, *BCS1L* mutations typically present as a failure to thrive with liver and kidney involvement, and lactic acidosis. However, some patients have shown central nervous system manifestations without obvious visceral phenotype.[92,93] In contrast to *MT-CYB* mutations, myopathy is an infrequent presentation of *BCS1L* mutations.

GRACILE syndrome is the most severe disease caused by *BCS1L* mutations.[16,94] It is also the most thoroughly characterized CIII deficiency (>40 patients). All the patients have had Finnish ancestry. The name of the syndrome derives from the main clinical features: growth restriction, aminoaciduria, cholestasis, iron overload in the liver, lactic acidosis, and early lethality. The growth restriction starts already during the fetal period and the patients are born small for the gestational age (-4 SD) and lack subcutaneous adipose tissue.[16,17,95] Clinical chemistry analyses show increased lactate concentration in the blood, and loss of amino acids, glucose and lactate into the urine. Typical histological findings are accumulation of bile acids, iron, and lipids in the liver. The iron accumulation is specific to liver and not present in other organs. The renal histology shows decreased number of proximal tubules with morphological alterations. The lifespan of the patients is from few days to few months. During the short lifespan, the patients do not show obvious central nervous system manifestations, although a few patients have shown atypical responses to sound stimulus, suggestive of Björnstad syndrome-type sensorineural hearing loss. All GRACILE syndrome patients have had the same Finnish founder mutation c.A232G (p.S78G). Outside Finland, other *BCS1L* mutations have caused GRACILE-like syndromes, however, without the full clinical picture of the GRACILE syndrome.[90,96,97]

6.4 Liver, the center of metabolism

6.4.1 Liver anatomy and physiology

Liver is the largest visceral organ.[98,99] It is located in the right upper abdominal cavity beneath the diaphragm. The lobes of the liver connect to hepatic artery, biliary tract, and portal vein. The portal vein brings low-oxygen nutrient-rich blood from the gastrointestinal tract to the liver. In contrast, the hepatic artery delivers oxygen-rich blood for the liver. Most water-soluble nutrients, xenobiotics and drugs undergo hepatic filtration before reaching other tissues. The biliary tract delivers bile acids to aid solubilization of dietary lipids in the small intestine.

The functional unit of liver is a liver lobule comprising a branch of the central vein surrounded by liver parenchyma, and multiple portal areas (Fig. 5).[98,99] Each portal area has three components: a branch of portal vein, arteriole(s), and bile duct(s). The direction of blood is towards the central vein through sinusoidal capillaries while the bile flows the opposite direction in the bile ductules. Microscopically, the liver appears relatively homogenous. However, a deep metabolite and oxygen gradient exist across the liver parenchyma.[100] Likewise, hepatocyte functions are regionally compartmentalized. For example, after feeding, the periportal hepatocytes conduct gluconeogenesis while the perivenous hepatocytes perform glycolysis. The bulk of the liver mass (~80%) is hepatocytes.

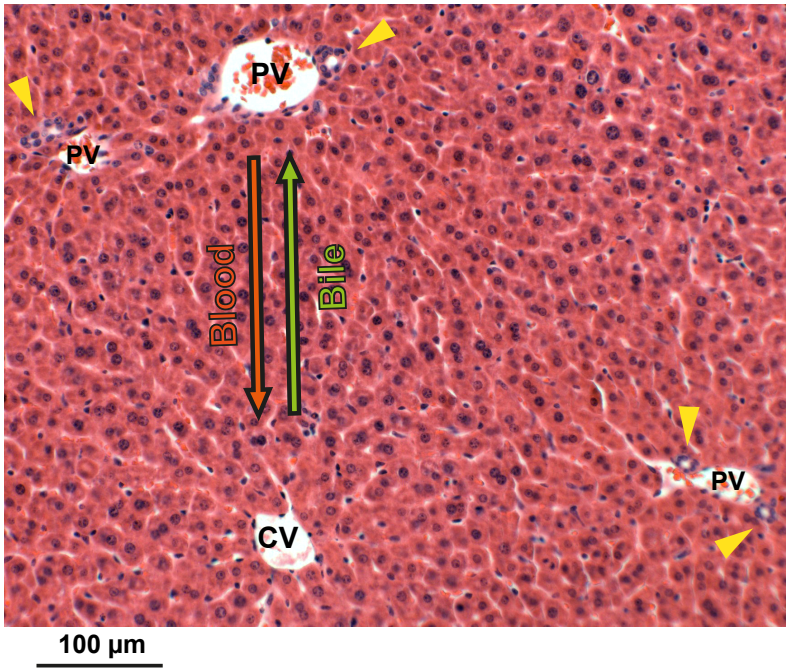

Figure 5. A cross-section of liver lobule stained with hematoxylin and eosin. CV, central vein; PV, portal venule. The direction of blood and bile are shown. Yellow arrow heads point to bile ducts and hepatic arterioles (small duct-like structures) next to PV.

Other abundant cells in the liver are cholangiocytes (bile duct epithelial cells), Kupffer cells (resident macrophages), stellate cells and sinusoidal endothelial cells.

Liver is undeniably the center of organismal metabolism.[98] It produces most of the circulating proteins in the blood such as albumin, transferrin, and lipoproteins. Approximately 40% of hepatic mRNA encode secreted proteins.[101] In addition, liver releases biosynthetic precursors such as cholesterol for other tissues. [98] Liver is also the main site of glycogen storage. Importantly, the hepatic glycogen is available for release into the circulation and serves as an important buffer for blood glucose. During fasting the hepatic glycogenolysis and gluconeogenesis become the main source of blood glucose. Liver also stores iron, copper, and vitamin A. Many vital detoxification processes including the urea cycle and the detoxification of xenobiotics takes place in the liver. Moreover, liver is an endocrine organ.[102] It secretes insulin-like growth factor and numerous hepatokines including stress-inducible hormones such as FGF21. In essence, liver is an organ that supports the maintenance of homeostasis in every tissue of the body.

6.4.2 Hepatic manifestations in OXPHOS disorders

An estimated 20% of neonatal OXPHOS defects manifest as hepatopathy.[103] Adult-onset mitochondrial hepatopathies are rare. Typical hepatic manifestations are steatosis, cholestasis, glycogen depletion, and hypoglycemia with lactic acidosis. Iron accumulation in hepatocytes and Kupffer cells is a hallmark of GRACILE syndrome but also present in some mtDNA depletion syndromes.[103–105] Hepatopathies related to isolated CI deficiency are virtually nonexistent in the literature. Hepatopathies due to isolated CIV deficiency are also rare and generally limited to the mutations in SCO1 involved in copper transfer to CIV.[106] The two major classes of mitochondrial hepatopathies are mtDNA depletion syndromes, and CIII deficiencies due to mutations in nuclear DNA-encoded subunits and assembly factors.[103] It remains unclear why these particular OXPHOS defects cause hepatopathy. According to animal models, insufficient mitochondrial ATP production or fatty acid oxidation appear not to be the sole factors. In mouse liver, disruption of mitochondrial fatty acid oxidation[107], membrane potential[108] or ADP/ATP exchange[109] does not cause overt liver damage under unstressed conditions.

6.5 Mouse models of CIII deficiency

A very limited repertoire of animal models exists for CIII deficiency. Full knock out of any subunit of CIII is likely embryonically lethal. Cell-type specific RISP and UQCRQ knock-out cells and mice have been utilized to investigate the role of respiratory electron transfer and CIII in cell differentiation[110], angiogenesis[111], hypoxia signaling[112] and adaptive immunity[113]. Mice carrying an artificial heterozygous RISP p.P224S mutation have been used to study aging but only minor sex-specific phenotypes were found.[114] Whole-body knock-out mice of TTC19[55] or PARL[115], needed for proteolytic processing of TTC19, are

viable, cause a mild CIII deficiency, and to some degree phenocopy the central nervous system manifestations of TTC19 mutations in patients. The only patient mutation animal model of CIII deficiency is the *Bcs1l*$^{p.S78G}$ knock-in mouse carrying the GRACILE mutation.[18]

6.5.1 *Bcs1l*$^{p.S78G}$ knock-in mouse model of GRACILE syndrome

The *Bcs1l*$^{p.S78G}$ mutant mice carry the same missense mutation as the GRACILE syndrome patients.[18] Unlike the patients, the *Bcs1l* mutant mice are born healthy but soon after weaning fail to grow and developed lactic acidosis, hypoglycemia, and liver and kidney disease. The CIII activity and the amount of fully assembled CIII are grossly normal at birth but gradually diminish coinciding with the appearance of the disease manifestations. Histologically the most affected organs are liver and kidney. The liver histology of the mutants shows periportal degenerating hepatocytes, glycogen depletion, and progressing fibrosis. The hepatic iron accumulation is less prominent than in the patients. The kidney histology shows decreased tubular mass and luminal casts suggestive of proteinuria. The lifespan of *Bcs1l*$^{p.S78G}$ mice ranges from 28 to 38 days on a Lund University C57BL/6JBomTac-derived background.[18,116,117]

6.6 Overview of strategies to improve dysfunctional mitochondria

Generally, there is no cure for mitochondrial diseases.[118,119] In a few special cases, a supplement can bypass the underlying defect such as in mitochondrial depletion syndrome due to thymidylate kinase 2 deficiency.[120] Gene therapy may be the only effective treatment for many mitochondrial diseases. However, many recent advances in the gene therapy field are valid only for the correction of nuclear DNA mutations. Targeting the multicopy mitochondrial genome is more challenging and the suggested tools are still in the very early stages of development.[118]

Preclinical interventions in animal models have given some hope that it may be possible to improve mitochondrial function in mitochondrial diseases.[118,119] One proposed approach is to increase mitochondrial biogenesis to compensate the dysfunctional mitochondria. Increased mitochondrial number is a frequent phenotype in some mitochondrial defects suggestive of an endogenous compensatory response.[104,121,122] Aberrant mitochondrial accumulation seen as ragged-red fibers is also a hallmark of mitochondrial myopathies.[123] Nevertheless, many mitochondrial diseases do not show increased mitochondrial biogenesis and may thus benefit from exogenous stimulation. Usually the strategies to increase mitochondrial biogenesis target metabolic regulators such as AMPK, sirtuin 1 (SIRT1), PPARα (peroxisome proliferator-activated receptor alpha) and PGC-1α (peroxisome proliferator-activated receptor gamma coactivator 1-alpha), which mediate adaptive mitochondrial responses.[118,119,124] Initially, PGC-1α overexpression-mediated increase in mitochondrial biogenesis proved beneficial in mouse models of CIV assembly defects.[125] PGC-1α is a master regulator of mitochondrial biogenesis.[124,126] It serves as a transcriptional

coregulator in induction of gene expression leading to enhanced oxidative metabolism in tissue- and isoform-specific manner.

Pharmacological PGC-1α activation strategies target AMPK and SIRT1 which activate it by phosphorylation and deacetylation, respectively.[118,119] AICAR (5-aminoimidazole-4-carboxamide ribonucleotide), an AMPK activator, has attenuated myopathy in four mouse models of CIV deficiency.[125,127] Cellular nicotinamide adenine dinucleotide (NAD^+) concentrations regulate SIRT1 deacetylase activity.[128] Inhibition of NAD^+ consuming processes (poly-ADP-ribose polymerases) or administration of NAD^+ precursors have also proven highly promising ways to attenuate secondary or primary mitochondrial dysfunction (section 6.8.3).[129–131] PGC-1α is a transcriptional coactivator for PPAR transcription factors.[132,133] The promoter of *PPARGC1A* gene encoding PGC-1α also contains a PPAR response element by which PGC-1α can upregulate its own expression. Therefore, PPAR agonists were thought to be efficient inducers of mitochondria biogenesis, and, indeed, a pan-PPAR agonist bezafibrate induces mitochondrial biogenesis in patient fibroblasts with different OXPHOS defects.[134] However, in mouse models of mitochondrial diseases, bezafibrate has mainly up-regulated fatty acid oxidation-related gene expression with both harmful and beneficial outcomes.[125,135,136] Nevertheless, an uncontrolled clinical trial on bezafibrate in mitochondrial myopathy was launched and its recent results suggest that the therapeutic effects are relatively modest.[137] At least four other clinical trials with mitochondrial biogenesis as a biochemical outcome parameter are also in progress.[118]

In contrast to SIRT1-AMPK-PGC-1α-axis activation, mtTOR pathway activation stimulates anabolic reactions.[138] The mtTORC1 inhibitor rapamycin has shown beneficial effects in several mouse models of mitochondrial diseases,[139–142] but it did not benefit mice with a coenzyme Q deficiency[143]. The exact mechanism of the beneficial effect is not yet clear, but induction of autophagy and clearance of dysfunctional mitochondria is one proposed mechanism.[140,141] Correction of aberrant mtTORC1 signaling in a mitochondrial myopathy model has also been suggested.[142]

6.7 Ketogenic diet

6.7.1 Ketosis

Ketosis is a physiological adaptation to prolonged starvation or lack of dietary carbohydrates.[144] A separate type of ketosis is the pathological ketoacidosis in diabetes.[145] In ketosis, repressed glucose utilization and increased fatty acid oxidation forces the liver to produce ketone bodies for those cells that cannot utilize fatty acids as an energy source.[144] β-hydroxybutyrate and acetoacetate are the relevant circulating ketone bodies, and they derive from the acetyl-CoA of fatty acid oxidation. The function of ketosis is to limit wasting of tissue protein for gluconeogenesis. Human brain can adapt to replace approximately 50% of glucose utilization with ketone bodies.[146] Gluconeogenesis in liver and to some degree in kidneys supply the residual glucose need.[147]

6.7.2 Composition of ketogenic diets

The classical ketogenic diet provides ~90% of energy as fat, sufficient amount of protein (typically 1 g / kg body weight), and minimal amount of carbohydrates.[144] In addition, several variations exist. Most of them are modified Atkins-type diets that have higher protein content than the classical ketogenic diet. Some ketogenic diet formulations contain high proportion of medium-chain triglycerides, which allows attenuation of carbohydrate restriction without the loss of ketogenesis.[148]

Commercial ketogenic rodent chows are also available for research purposes. The achievement of dietary ketosis in rodents requires strict restriction of not only carbohydrates but also protein.[149] The protein restriction has proven problematic in some cases, and one widely used commercial ketogenic chow causes hepatotoxicity and weight loss linked to overt choline and methionine deficiency.[150,151] This problem is rarely discussed and many studies do not report adequately the composition or commercial source of the chow to allow evaluation of whether the noted effects are due to nutritional ketosis or malnutrition. As an example, some studies have attributed over 40-fold upregulation of hepatic *Fgf21* expression as an effect of ketogenic diet,[152] when in fact the same diet supplemented with methionine induces *Fgf21* expression only minimally.[151] FGF21 is a marker for mitochondrial diseases but also an important endocrine regulator in fasting and feeding responses in normal physiology.[153] Another potentially relevant parameter in ketogenic diets is the fat source. Dietary fatty acid composition affects the mitochondrial phospholipid acyl chain profile, including that of cardiolipin to some degree.[154,155] Moreover, some metabolites of the unsaturated fatty acid metabolism are ligands for PPAR transcription factors.[156]

6.7.3 Ketogenic diet as a therapy for mitochondrial disease

The regulation of mitochondrial biogenesis, dynamics and function are inherently linked to starvation signals that aim to enhance OXPHOS efficacy during energy scarcity.[21,157] Accordingly, fasting and caloric restriction can cause beneficial mitochondrial changes in animal models and humans.[158–160] Ketogenic diet has a long history as a mimetic of anti-epileptic starvation ketosis in the management of epilepsy.[161] The mechanism of action of ketogenic diet in epilepsies is unknown but involvement of an adaptive mitochondrial response has been proposed.[162] In mitochondrial diseases, ketogenic diets may also relieve dependence on anaerobic glycolysis by forcing the cells to oxidize fatty acids and ketone bodies.[162,163]

The first demonstration of the beneficial effect of ketone bodies in mitochondrial dysfunction came from cybrid cells with mtDNA deletions in which ketone body supplemented-media shifted heteroplasmy towards wild-type mtDNA.[164] The authors of this study presented evidence suggesting intracellular selection for wild-type mtDNA upon ketone body treatment. An independent study has confirmed the attenuation of mtDNA mutation load in patient cell lines.[165] In a neuronal cell line carrying essentially homoplasmic MELAS (mitochondrial encephalomyopathy, lactic acidosis, and stroke-like episodes) mutation,

ketone bodies increased mtDNA amount and restored CI assembly defect.[166] In contrast, in a mouse model of myopathy with progressive accumulation of mtDNA deletions due to mutated mitochondrial TWINKLE helicase, ketogenic diet did not affect mtDNA mutation load or amount.[167] However, ketogenic diet decreased the number of cytochrome oxidase-negative muscle fibers, normalized mitochondrial structural aberrations, and increased mitochondrial mass according to citrate synthase activity. In a mouse model of mitochondrial translation deficiency, ketogenic diet has also ameliorated OXPHOS defects, especially in the liver.[168] Correction of mtTOR pathway hyperactivity and increase in AMPK signaling accompanied the beneficial effect. A rather different outcome took place in a mouse model of mtDNA depletion syndrome ($MPV17^{-/-}$) in which ketogenic diet caused liver failure.[55] However, this report did not disclose the chow composition or source and therefore it remains unclear whether the diet caused a choline and methionine deficiency.

Clinical trials on ketogenic diet in mitochondrial diseases are scarce. Ketogenic diet is an approved therapy for drug-resistant epilepsy[169], pyruvate dehydrogenase[170] and glucose transporter 1[171] deficiencies. A retrospective uncontrolled cohort study also suggests ketogenic diet as an efficient and relatively safe therapy for epilepsies caused by primary OXPHOS defects.[172] In mitochondrial myopathy patients (primary or secondary mtDNA deletions), ketogenic diet caused acute muscle pain that lead to premature discontinuation of the intervention.[173]. However, the cell lysis behind the muscle pain appeared to be selective for ragged-red fibers, muscle fibers with the accumulation of aberrant mitochondria. A single case report described a partial recovery of alopecia with unaffected progression of sensorineuronal hearing loss in CIII deficiency (Björnstad syndrome) on ketogenic diet.[174]

In addition to putative starvation-like adaptive response targeting mitochondria, ketogenic diet may also have other mechanisms of action. Ketone bodies have themselves endogenous signaling functions. The main circulating ketone body β-hydroxybutyrate inhibits NRLP3 inflammasome activation[175] and is an endogenous ligand for the niacin receptor HCAR2 (GPR109A)[176]. β-hydroxybutyrate is also a proposed histone deacetylase inhibitor,[177] although not all studies agree.[178] The signaling functions of β-hydroxybutyrate in the context of mitochondrial dysfunction, however, remain unstudied.

6.8 Targeting NAD^+ metabolism in mitochondrial dysfunction

6.8.1 NAD^+ in cellular metabolism and signaling

Nicotinamide adenine dinucleotide (NAD^+) is a ubiquitous vital cellular electron-carrying coenzyme of oxidative metabolism.[128] OXPHOS, or lactate production and excretion, maintains its reduced form (NADH) at low concentration The reduction-oxidation reactions of oxidative metabolism recycle the NAD^+/NADH pair but do not consume the NAD^+ molecule. The processes that consume NAD^+ are not directly involved in energy metabolism but in cellular signaling, protein posttranslational modification, and DNA damage response.[128] In addition, NAD^+ is a precursor for the biosynthesis of NADPH

(reduced nicotinamide adenine dinucleotide phosphate), an important source of reducing equivalents required for biosynthetic reactions and maintenance of cellular antioxidant systems. Four known NAD^+ consuming enzyme families exist in mammals: sirtuins (SIRT1-SIRT7)[179], ADP-ribose transferases and polymerases (PARP1- PARP17)[180], CD38 and CD157 NAD^+ hydrolases[181], and SARM1 NAD^+ hydrolase[182]. The sirtuin family members SIRT1 and SIRT3 are especially important in the regulation of mitochondrial function.[128] They serve as NAD^+-dependent lysine deacetylases and NAD^+ concentration is likely rate limiting for their activity based on Michaelis-Menten constant for NAD^+. SIRT1 localizes predominantly to nucleus and deacetylates a number of lysine residues in transcriptional regulators including in PGC-1α.[128,183] SIRT3 is a mitochondrial deacetylase with numerous substrates including several respiratory complex subunits.[179] In contrast to enzymatic protein acetylation in the nucleus and cytoplasm, protein acetylation in mitochondrial matrix is a constant nonenzymatic process due to high pH and high concentration of acetyl-CoA.[184,185]

6.8.2 NAD^+ biosynthesis

The vitamin B3s nicotinic acid (niacin) and nicotinamide are the classical NAD^+ precursors.[128] Nicotinamide is also the product of all NAD^+ consuming processes and salvageable to NAD^+ in most cells. Nicotinamide is two enzymatic steps away from NAD^+ (Fig. 6). The rate-limiting enzyme in the NAD^+ salvage is nicotinamide phosphoribosyltransferase (NAMPT), which inhibition[186] or overexpression[187] alters cellular NAD^+ concentrations. Endogenously, NAMPT is under transcriptional regulation by clock genes and SIRT1, giving circadian rhythm to cellular NAD^+ levels.[188,189]

Gut microbiota affects NAD^+ metabolism by metabolizing a large proportion of dietary nicotinamide to nicotinic acid.[190] Both of these NAD^+ precursors are highly bioavailable, but different pathways conduct their conversion to NAD^+ in tissue-specific manner (Fig. 6).[191,192] The Preiss-Handler pathway enzymes, mainly in gut epithelia, liver and kidney, metabolize nicotinic acid to NAD^+, which will eventually undergo conversion to nicotinamide (Fig. 6). By contrast, nicotinamide is the main circulating NAD^+ precursor and the main substrate for NAD^+ biosynthesis in most tissues including skeletal muscle, heart, adipose tissue and central nervous system.[191,192] In addition, some tissues, primarily liver and kidney, can synthetize the pyridine ring of NAD^+ *de novo* from tryptophan for the biosynthesis of nicotinic acid mononucleotide which joins the Preiss-Handler pathway in the NAD^+ biosynthesis.[192] Liver plays an important role in whole body NAD^+ metabolism by releasing nicotinamide for NAD^+ biosynthesis in extrahepatic tissues.

A reinvestigation of NAD^+ biosynthetic routes in 2004 led to a discovery of a novel vitamin B3, nicotinamide riboside (NR).[193] NR has some potential advantages over nicotinic acid and nicotinamide when the aim is to increase cellular NAD^+. First, large doses of nicotinic acid cause cutaneous vasodilation observed as redness and heat due to stimulation of HCAR2 receptor.[194] NR and nicotinamide do not stimulate HCAR2.[129] Second, NR, being already ribosylated, can bypass a rate-limiting step catalyzed by NAMPT (Fig. 6), which

is also under positive feedback inhibition by NAD^+.[193,195] Third, nicotinamide is a product of NAD^+ consuming reactions and serves as negative feedback inhibitor for sirtuins.[196] However, recent NAD^+ metabolite flux analyses have shown that enterohepatic metabolism converts almost all orally administered NR to nicotinamide.[190,192] Moreover, NR degrades to nicotinamide within minutes in whole blood.[192,197] The same is true for intravenously administered phosphorylated NR (nicotinamide mononucleotide, NMN).[192] Interestingly, the reduction of NR to dihydro-NR (NRH) slows down the cleavage to nicotinamide, which renders NRH a more potent enhancer of cellular NAD^+ levels in culture and *in vivo* than NR.[197–199] However, NRH is still a very recent innovation as a NAD^+ precursor and little studied.

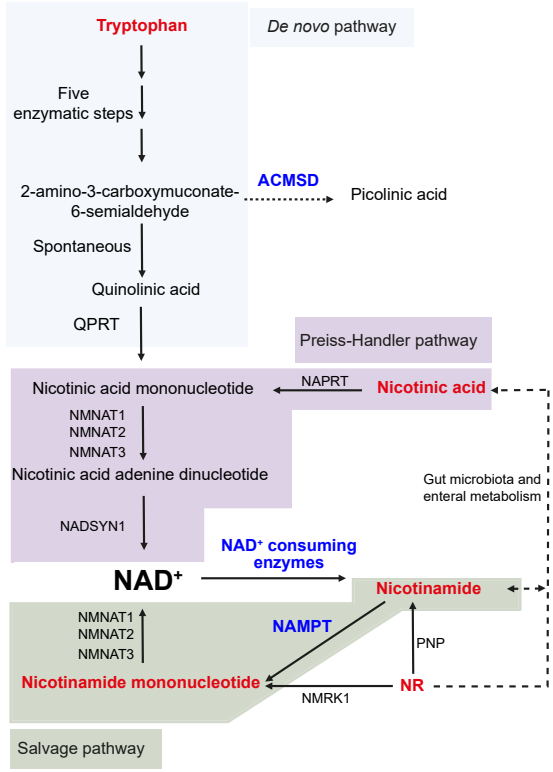

Figure 6. NAD^+ biosynthetic pathways. Molecules referred with red text indicate NAD^+ precursors that can be administered to increase NAD^+ biosynthesis. The enzymes involved are marked next to the arrows using their official gene symbols. The enzymes that can be pharmacologically targeted are marked with blue-colored text. NR, nicotinamide riboside.

6.8.3 NAD^+-repletion therapies

Vitamin B3 and tryptophan deficiency causes pellagra, a potentially lethal condition characterized by photosensitive dermatitis, diarrhea, and dementia.[200] Relatively recently, a secondary NAD^+ depletion not related to malnutrition or malabsorption has been found in animal models of different metabolic conditions.[201–205] Usually, NAD^+ depletion involves a repression of mitochondrial respiratory activity. The aim of NAD^+-repletion therapies is to normalize cellular NAD^+ concentration and typically enhance mitochondrial function by targeting the NAD^+-dependent metabolic regulators SIRT1 and SIRT3.[128] The cellular NAD^+ concentration can be increased by promoting its biosynthesis or by decreasing its consumption (Fig. 6).

The preclinical interventions have mainly utilized the novel NAD^+ precursors NR and NMN to promote NAD^+ biosynthesis.[129–131,201,203,204,206,207] However, rarely have the studies included a side-by-side comparison to nicotinic acid or nicotinamide. Two experimental drugs also exist to target key enzymes in NAD^+ biosynthesis. Inhibition of ACMSD, an enzyme that channels a vital intermediate of tryptophan catabolism away from NAD^+ biosynthesis, normalized hepatic NAD^+ levels in mice fed methionine- and choline-deficient diet.[205] A small-molecule NAMPT activator also exists but its effects in disease models are still unreported in the literature.[195] An alternative approach to increase cellular NAD^+ levels is to inhibit the NAD^+ consuming processes, mainly PARP1 and CD38. Inhibition of either of the enzymes in mice shows increased cellular NAD^+, enhanced activity of SIRT1 and OXPHOS.[181,203,208] However, the importance of PARP1 in DNA repair likely limits the usability of its inhibitor in humans. CD38 has immunomodulatory functions and its pharmacological inhibition are unstudied in disease models.

By now, the so-called NAD^+-boosting therapies have been studied in more than 30 rodent disease models with mostly beneficial outcomes.[128] However, the first randomized controlled clinical trials on NR in insulin-resistant obese[209], and in elderly men[210], have not shown prominent effects on skeletal muscle mitochondrial function or NAD^+ levels. In two mouse models of mitochondrial myopathy, NAD^+-based therapy ameliorated the disease. Cerutti et al. showed that PARP1 inhibition or NR supplementation for 4 weeks increases skeletal muscle respiratory enzyme activities and improves exercise tolerance in mice with mutated CIV assembly factor SCO1.[130] They also found that NR increased NAD^+-to-NADH ratio in skeletal muscle while mtDNA content and citrate synthase activity, markers of mitochondrial mass, remained unchanged. Khan et al. investigated a longer, 16-week, NR treatment on a late-onset mitochondrial myopathy model with progressive mtDNA deletions.[131] They found attenuation of multiple hallmark phenotypes of the model: decreased mtDNA mutation load and number of cytochrome c oxidase-negative muscle fibres, and increased mitochondrial cristae density. Whether NR increased the NAD^+ levels in this model remains unclear but increased citrate synthase activity and respiratory enzyme proteins suggested increased mitochondrial mass due to the NR supplementation. In CI-deficient mice (*Ndufs4* knockout), intraperitoneally administered NMN has extended the survival of the knockout mice. In this model, NMN administration repleted cellular NAD^+ in skeletal muscle, but not in liver, heart or brain of the knockout

mice. The beneficial effects in myopathic mice provided a basis for an uncontrolled clinical trial on nicotinic acid supplementation in mitochondrial myopathy patients.[211] The patients showed low baseline whole blood and skeletal muscle NAD^+ levels that were improved after 4 and 10 months of supplementation. At the end of the follow-up mtDNA amount and mutation load, and structural aberrations of mitochondria were similar to the baseline. However, the number of cytochrome c oxidase-negative muscle fibers had decreased, suggesting improved OXPHOS.

6.9 Xenogenic alternative oxidase expression in mammalian cells, and mice

Mammalian mitochondria have only one quinol oxidase (CIII) and only one terminal oxidase (CIV). Some lower animals, plants and fungi, however, have alternative oxidases (AOXs) that can bypass the CIII-CIV segment of respiratory electron transfer (Fig. 7).[212] In these organisms, AOXs are mostly not constitutively active but take over the respiration under specific conditions that likely involve an accumulation of reduced coenzyme Q.[212,213] In addition, some blood-borne parasites such as *Trypanosoma brucei*, causative for sleeping sickness, utilize AOX to speed-up aerobic glycolysis.[214] As AOX bypasses two out of three proton translocases (CIII and CIV) in the OXPHOS, respiring on AOX is a relatively inefficient way of generating ATP.

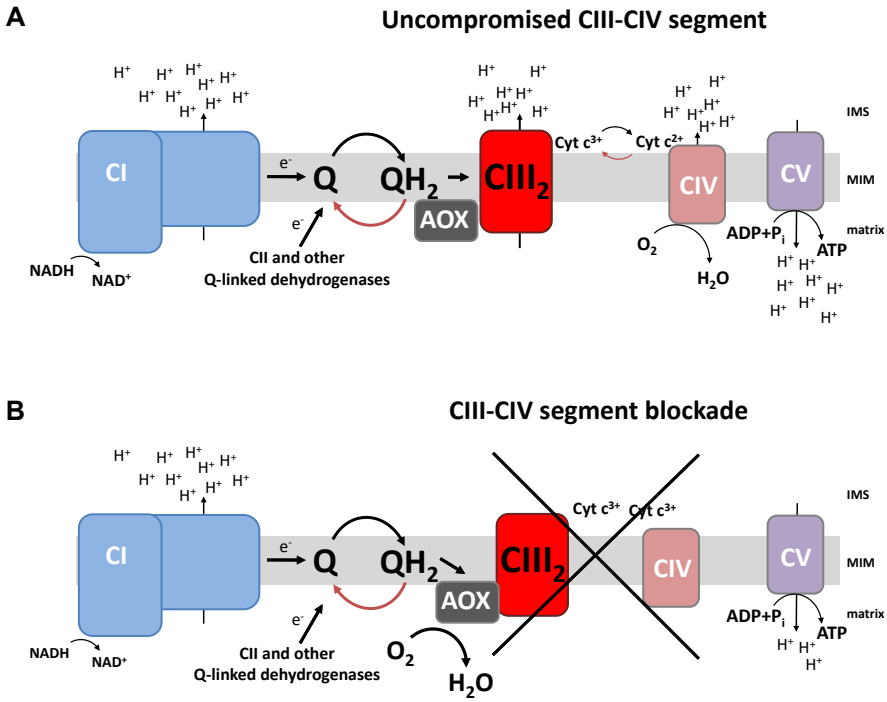

Figure 7. Alternative oxidase (AOX) in respiratory-electron transfer. (**A**) In uncompromised respiratory-electron transfer, CIII outcompetes AOX in ubiquinol (QH_2) oxidation. (**B**) Upon CIII-CIV segment insufficiency, AOX oxidizes ubiquinol and reduces oxygen to water bypassing CIII and CIV.

Transgenic AOXs from the tunicate *Ciona intestinalis* and the fungi *Emericella nidulans* have been studied in several mammalian cell lines[27,215–217] and also in mice[218,219]. These enzymes correctly localize to mammalian mitochondrial inner-membrane and restore respiration upon the blockade of the CIII-CIV segment of the electron transfer. With uncompromised CIII and CIV AOXs remain largely inert.[218,219] Healthy mice expressing AOX show no obvious phenotype except the expected resistance to CIII and CIV inhibitors.[218,219] AOXs have proven useful mechanistic tool to study the role of different segments of the respiratory electron transfer for example in mitochondrial ROS production[65]. In mtDNA depleted cells, AOX can restore uridine auxotrophy by allowing the enzymatic activity of coenzyme Q-dependent DHODH.[27,220] Under certain circumstances, AOXs can also alter hypoxia responses[221], and prevent succinate accumulation-related ROS signalling[222].

7 AIMS OF THE STUDY

The aim of this thesis was to elucidate disease mechanisms in CIII-deficiency by means of dietary, pharmacological, and genetic interventions, with an emphasis on relevance to therapy development. The main organ of interest was the liver. The fourth study arose from an unexpected identification of a novel mouse mtDNA variant. The specific aims were:

1) To study the effect of ketogenic diet on mitochondrial hepatopathy in *Bcs1l*$^{p.S78G}$ mice.

2) To characterize NAD^+ metabolism and signaling, and the effect of NAD^+-precursor therapy in *Bcs1l*$^{p.S78G}$ mice

3) To study AOX-mediated restoration of electron transfer upstream of CIII in *Bcs1l*$^{p.S78G}$ mice.

4) To characterize the effect of *mt-Cyb*$^{p.D254N}$ variant on *Bcs1l* wild-type and mutant mice.

8 METHODS

The original publications describe the methods (Table 1) in detail. Here, the design of the studies and the animal experiments are summarized.

8.1 Mouse strains and ethics

We studied the *Bcs1l*$^{p.S78G}$ knock-in mice[18] on two different congenic backgrounds. In University of Helsinki, the mice were on C57BL/6JCrl (Study **I**, **II**, **III**, **IV)** and in Lund University on a local C57BL/6JBomTac-derived background (**II**). In study **IV**, we also generated F1 hybrid mice from these two substrains. Both female and male mice were used in the experiments.

The Animal Experiment Board, Finland (ELLA) authorized the animal experiments in Helsinki under the permits: ESAVI-2010-07284/Ym-23, ESAVI/6142/04.10.07/2014 and ESAVI/6365/04.10.07/2017. The experiments in Sweden were performed under the Lund University/M124-15 licence. All animal experiments and reporting were carried out in accordance to the FELASA (Federation of Laboratory Animal Science Associations) and ARRIVE (Animal Research: Reporting of In Vivo Experiments) guidelines.

8.2 Monitoring of condition of *Bcs1l*$^{p.S78G}$ homozygotes

We used a semi-quantitative scoring system[116] based on behavioral changes and weight loss to minimize the suffering of the mice, and to prevent spontaneous deaths, and to estimate survival. The behavioral scoring comprises six parameters: waddling gait, reduced curiosity, lack of movement, kyphosis, loss of balance, and loss of grip strength. Each parameter was scored on a 3-point scale (0, normal; 1, moderate; 2 severe). If the mice reached a total score higher than 7 or weight loss more than 20%, they were euthanized. For survival analyses, the personnel performing the scoring were unaware of any group allocations.

8.3 Ketogenic diet intervention

The control mice received a cereal and soy-based rodent chow (Teklad 2018, Harlan). Its macronutrient energy composition (% of energy, E%) was 18 E% fat, 58 E% carbohydrates, and 24 E% protein. The ketogenic chow was based on vegetable oils (soybean, palm and corn oil) and casein. It provided 90.5 E% fat, and 9.1 E% protein. The fatty acid profile of the chow was following: 21 E% saturated fatty acids, 35 E% monounsaturated fatty acids, 30 E% linoleic acid, and 2.5 E% linolenic acid. Both chows contained standard vitamin and mineral supplements and provided similar amount of choline (~8.5 mg/100kJ) and methionine (~30 mg/100kJ). All mice were familiarized to the ketogenic chow in the presence of standard chow before weaning. After weaning (3 weeks of age), the litters received *ad libitum* control or ketogenic chow only. One experimental set of mice was

euthanized after 3 weeks (n=11-14/group). A second interventions lasted for 10 weeks (n=8-9/group).

8.4 NR supplementation

Randomized *Bcs1l*$^{p.S78G}$ homozygotes and their heterozygous or wild-type littermates received either control chow (Teklad 2018, Harlan) or the same chow supplemented with NR (2.4 g/kg chow) starting at weaning. The estimated NR dosage was 400 mg/kg body weight. Novalix Pharma (Strasbourg, France) custom synthetized the NR as a trifluoromethanesulfonate (triflate) salt. Several previous studies have used the same NR formulation.[129,130,201] The mice were followed for 3 months in Helsinki (C57BL/6JCrl background) (n=8/group) and until the development of terminal stage in Lund University (C57BL/6JBomTac-derived background) (n=5-6/group).

8.5 AOX-expressing mice

We crossbred *Ciona intestinalis* AOX transgenic mice[219] with *Bcs1l*$^{p.S78G}$ heterozygotes to obtain suitable breeding mice to produce *Bcs1l*$^{p.S78G}$ homozygotes with and without heterozygous AOX transgene. Wild-type and heterozygous *Bcs1l*$^{p.S78G}$ littermates were used as healthy controls. The AOX transgene is in the Rosa26 locus and it is ubiquitously transcribed under a strong synthetic CAG promoter.[219] In the original publication, the *Bcs1l*$^{p.S78G}$ homozygotes are referred as GRAC (GRACILE) and when they express AOX as GROX (GRACILE + AOX).

The experimental cohorts of mice comprised four genotypes: 1) wild-type (WT), 2) *Bcs1l*^{WT};*Rosa26*^{AOX}, 3) *Bcs1l*$^{p.S78G}$ and 4) *Bcs1l*$^{p.S78G}$;*Rosa26*^{AOX}. We used one set of mice (n= 18-21/genotype) to estimate the lifespan. Two other sets of mice were euthanized at 5 and 6.5 month of age to collect samples prior and at the terminal stage of the *Bcs1l*$^{p.S78G}$ homozygotes, respectively. In addition, we transferred one experimental cohort to German Mouse Clinic (www.mouseclinic.de) for phenotype screening between ages of 56 and 112 days (n=20/genotype).

8.6 Lund University 6JBomTac and Harlan 6JCrl hybrid mice

To generate mice differing in their mtDNA but having equalized nuclear DNA, we crossbred *Bcs1l*$^{p.S78G}$ heterozygotes from congenic Lund University C57BL/6JBomTac and commercial C57BL/6JCrl (Harlan) substrains. Given the congenic nature of the substrains, the outcome of this crossbreeding experiment was first generation (F1) hybrid mice having the parenteral homozygous nuclear DNA differences in a heterozygous state and the mtDNA determined by the maternal background. Subsequently, we backcrossed the Lund University C57BL/6JBomTac mtDNA genome onto the C57BL/6JCrl nuclear background for independent replications of the key parameters.

Table 1. List of methods

Method		Study
Histochemistry		
	Paraffin-embedded sections	**I, II, III, IV**
	Cryosections	**I**
	Hematoxylin and eosin	**I, II, III IV**
	Periodic acid-Schiff	**I, II, IV**
	Sirius Red	**I, II, III IV**
	Oil-Red-O	**I**
	DAB-enhanced Prussian Blue	**II**
	Immunostaining	**I, II, III IV**
	Automated image quantification	**I, II, III, IV**
Electron microscopy		**I, III**
Clinical chemistry		
	Blood glucose	**I, II, III, IV**
	Blood lactate	**I**
	Blood β-hydroxybutyrate	**I**
	Plasma liver enzyme activities	**I, II, III**
	Urine albumin and creatinine	**III**
	Echocardiography	**III**
Protein analyses		
	SDS-PAGE and Western Blot	**I, II, III, IV**
	Blue-Native PAGE and Western blot	**I, III, IV**
	Proteomics	**II**
	Mitochondrial enzyme activity measurements	**I, II, III, IV**
	Molecular dynamics simulations	**IV**
	Pulse EPR spectroscopy	**IV**
Gene expression analyses		**I, II, IV**
	qPCR	**I, II, IV**
	Transcriptomics	**I, II*, III**
Whole genome sequencing		**IV**
Lipid analyses		
	Liver triglycerides	**I**
	Liver free fatty acids	**I**
Metabolite analyses		
	Plasma metabolomics	**I, II**
	Liver metabolomics	**II*, III**
	ATP measurements	**IV**
	NAD^+ and NADH measurements	**II**
Mitochondrial respirometry		**II, III, IV**
Measurement of mitochondrial H_2O_2 emission		**III, IV**
Indirect calorimetry (CLAMS)		**III, IV**

* Transcriptomics and metabolomics data from studies **I** and **III** were also utilized in the study **II.**

9 RESULTS AND DISCUSSION

9.1 mtDNA background alters the disease course of *Bcs1l*$^{p.S78G}$ mice (Studies I-IV)

The *Bcs1l*$^{p.S78G}$ knock-in mutant mice were generated and characterized in mixed 129/SvEvTac:C57BL/6 as well as on an in-house congenic C57BL/6JBomTac-derived background in Lund University, Sweden.[18,116,223] For the studies **I**-**IV**, we transferred heterozygous *Bcs1l*$^{p.S78G}$ embryos to University of Helsinki and backcrossed the mutation into a commercial C57BL/6JCrl substrain. The early-onset phenotypes of the homozygotes were similar as described in Lund University. However, to our surprise, the homozygotes survived the early-onset metabolic crisis at one month of age. In studies **I** and **III**, we characterized the novel late-onset phenotypes. The study **IV** identified a novel mtDNA variant (*mt-Cyb*$^{p.D254N}$) in the original Lund University mouse colony as the determinant of the short lifespan of the *Bcs1l*$^{p.S78G}$ homozygotes.

9.2 Ketogenic diet attenuates CIII deficiency-related hepatopathy (I)

Ketogenic diet has been suggested to induce a starvation-like adaptive response leading to enhancement of mitochondrial function.[162,163] Based on positive findings in cell culture models[164–166] and in a mitochondrial myopathy model[167], we set out to test ketogenic diet as a therapy for CIII deficiency-related hepatopathy.

9.2.1 Bcs1l$^{p.S78G}$ mice tolerate carbohydrate restriction and readily sustain nutritional ketosis

Hypoketotic hypoglycemia is a phenotype of *Bcs1l*$^{p.S78G}$ mice.[117,158] Therefore, we hypothesized that ketogenic diet could decrease the dependence on glycolysis by forcing the cells to use fatty acids and ketone bodies. On the other hand, CIII deficiency may compromise mitochondrial fatty acid oxidation, which could render the mice intolerant to a high-fat ketogenic diet.[223] We found that the *Bcs1l*$^{p.S78G}$ mice readily adapted to ketogenic diet as shown by the induction of ketogenesis and the maintenance of blood glucose at a similar level as on standard chow (**I**, Table 2). Ketogenic diet also did not affect the growth of mutant mice (**I**, Supplementary Fig.1). In wild-type mice, ketogenic diet induced ketosis during the juvenile period (<P50) (**I**, Table1), whereas adult mice exposed for approximately 10 weeks to ketogenic diet were no longer in ketosis. The lack of sustained ketosis in wild-type mice was likely due to the relatively mild protein restriction, as dietary protein inhibits ketosis in rodents.[149] *Bcs1l*$^{p.S78G}$ mice responded differently. They remained in ketosis during the whole follow-up (β-hydroxybutyrate, >4.5 mM).

9.2.2 Ketogenic diet attenuates markers of acute and chronic liver damage

During study **I**, we extended the characterization of the liver pathology of *Bcs1l*$^{p.S78G}$ mice. Liver disease progression was also the primary outcome for the ketogenic diet intervention. Table 2 summarizes the findings and the effect of ketogenic diet. Ketogenic diet attenuated most of the histopathological findings including fibrosis, stellate cell activation, hepatocyte death, and hepatic progenitor cell response (**I**, Fig. 1-2). The liver enzyme activities in plasma were also attenuated (**I**, Table1). As expected, ketogenic diet did not improve glycogen depletion (**I**, Supplementary Fig. 2). Ketogenic diet increased liver triglyceride content in wild-type and mutant mice but did not cause overt steatosis (**I**, Fig 1F). It is of note that some ketogenic diet formulations do cause pathological steatosis in mice due to insufficient choline and methionine content.[150,151]

Table 2. Effect of ketogenic diet on liver disease progression in *Bcs1l*$^{p.S78G}$ mice

Parameter	Effect of ketogenic diet
Liver histology	
Fibrosis	↓
Stellate cell activation	↓
Cellular death	↓
Hepatic progenitor cell response	↓
Lipofuscin/ceroid accumulation	↓
Gylcogen depletion	↑
Plasma clinical chemistry	
Aminotransferase	↓
Alkaline phosphatase	↓
Hypoglycemia	no change

One of our novel histological findings was hepatic progenitor cell response in mutant mice (**I**, Fig. 1A, Fig. 2A, and Supplementary Fig. 4). In the literature, this finding is also described as oval cell hyperplasia or ductular reactions.[224] Its presence correlates with the severity of hepatopathy in humans.[225] In experimental models, liver regeneration does not evoke an overt hepatic progenitor cell response unless a simultaneous cytotoxic insult or hepatocyte senescence is present.[226,227] Of note, the livers of *Bcs1l*$^{p.S78G}$ mice accumulated ceroid-lipofuscin-like material suggesting increased cellular senescence, which was attenuated by ketogenic diet (**I**, Supplementary Fig 12). Normally liver regenerates by hypertrophy and proliferation of hepatocytes with little contribution from the progenitor cells.[226] Therefore the results suggest that the hepatocytes of *Bcs1l*$^{p.S78G}$ mice were prone to senescence and had insufficient mitotic capacity. The hepatic progenitor cell response is visible in H&E-stained sections as expansion of non-parenchymal cells with oval-like morphology. Occasionally these cells form bile duct-like structures (ductular reactions) outside portal areas. As the hepatic progenitor cells are able to differentiate into

hepatocytes and cholangiocytes, they express antigens of both compartments, which allows their visualization by immunostaining against bile duct markers such as cytokeratin-7. Importantly, ketogenic diet essentially prevented the formation of ductular reactions and aberrant cytokeratin-7 immunoreactivity at juvenile period (postnatal days 40-45, P40-45) and significantly decreased them at a later time point (P95) (**I**, Fig. 1A, Fig 2A).

9.2.3 Ketogenic diet partially normalizes hepatic mitochondrial structure and function

As ketogenic diet has been suggested to increase mitochondrial biogenesis,[162,167] we quantified the hepatic expression of *Ppargc1a* (encoding PGC-1α) and genes encoding for mitochondrial proteins (**I**, Fig 4G,I and Supplementary Fig. 8). To assess relative mitochondrial mass, we quantified mtDNA copy number, citrate synthase activity and amounts of several mitochondrial proteins (**I**, Fig 4A-C). None of these indicated that ketogenic diet increased mitochondrial biogenesis in the liver. However, PGC-1α was induced at mRNA level in the mutant mice independently of the diet, as was citrate synthase activity, and some mitochondrial proteins in liver lysates, suggesting increased mitochondrial content. In contrast, ketogenic diet increased skeletal muscle citrate synthase activity, a commonly used mitochondrial marker enzyme, as also reported in a mitochondrial myopathy model[167]. However, ketogenic diet did not increase mitochondrial protein levels in muscle homogenates, suggesting unaltered mitochondrial mass.

Despite no evidence of increased mitochondrial biogenesis, ketogenic diet improved the assembly and activity of CIII in liver mitochondria (**I**, Fig. 3, Fig. 4F-F). Previously, in cultured cells with a homoplasmic mutation affecting mitochondrial leucine tRNA, ketone bodies improved assembly and activity of CI.[166] In these cells, the improvement could have been due to an increase in mtDNA copy number. In the case of nuclear *Bcs1l* mutation, the mechanism remains elusive. A robust normalization of mitochondrial ultrastructure by ketogenic diet, however, indicated a global improvement in mitochondrial condition (**I**, Fig. 3). Ketogenic diet has also corrected mitochondrial morphology in a mouse model of myopathy.[167] Several studies have demonstrated that mitochondrial function and morphology are tightly connected.[228–230]

9.2.4 Mechanistic insights from liver transcriptomics

To gain deeper understanding of the effect of ketogenic diet and the *Bcs1l*$^{p.S78G}$ mutation, we performed liver transcriptome analysis. Many of the most upregulated genes due to the *Bcs1l*$^{p.S78G}$ mutation were related to macrophage activation and glutathione-mediated detoxification (**I**, Fig. 6 and 7). Ketogenic diet normalized several of these changes. Moreover, immunohistochemical analyses showed a clear change in macrophage populations and morphology in the *Bcs1l*$^{p.S78G}$ mutants, and attenuation by ketogenic diet (**I**, Fig. 2). The polarization of macrophages into different subclasses involves a large shift

in energy metabolism and mitochondrial function.[222] The proinflammatory, classically activated, M1 macrophages are highly glycolytic whereas the alternatively activated, anti-inflammatory, M2 macrophages use OXPHOS. Macrophage polarization in the context of CIII deficiency is a largely unstudied topic, but, for example, a loss of complex I activity in mice can cause systemic inflammation[231], and the complete loss of CIII activity in regulatory T cells is sufficient to cause lethality in mice[232]. Interestingly, liver macrophages express the β-hydroxybutyrate receptor HCAR2, and β-hydroxybutyrate administration has ameliorated acute liver toxicity by promoting M2 macrophage polarization via HCAR2-mediated signaling.[233] In addition, β-hydroxybutyrate modulates macrophage activation and suppresses inflammation by inhibiting NLRP3 inflammasome activation.[175]

The transcriptome data also predicted repressed tryptophan catabolism and the related NAD^+ *de novo* biosynthesis. We investigated these changes further in study **II**.

9.3 NAD^+ metabolism in CIII-deficient mice (II)

When we initiated this study in 2014, non-pellagra metabolic NAD^+ depletion was a recently recognized condition and the NAD^+-repletion therapies were just emerging. Promising results with the NAD^+ precursor NR in two mouse models of mitochondria myopathy[130,131] prompted us to study NAD^+ metabolism in a CIII deficiency-related hepatopathy.

9.3.1 Repressed NAD^+ biosynthesis and NAD^+ depletion in *Bcs1l*$^{p.S78G}$ mice

In study **I**, we found hepatic gene expression changes in young (P45) *Bcs1l*$^{p.S78G}$ mice suggesting repressed tryptophan catabolism and nicotinic acid utilization for NAD^+ biosynthesis. These changes were also present in older (P150) mutant mice in the liver but also in the kidney (Fig. 8) (**II**, Fig. 1). Liver and kidney are the main organs utilizing tryptophan and nicotinic acid for NAD^+ biosynthesis.[190–192] Endogenously, other tissues rely mainly on nicotinamide as a NAD^+ precursor. In contrast to the transcriptionally repressed *de novo* NAD^+ biosynthesis, the gene expression of the rate-limiting enzyme, *Nampt*, in the NAD^+ salvage from nicotinamide was increased in the liver and kidney, suggesting heightened need for NAD^+. Indeed, we found decreased hepatic NAD^+ levels in *Bcs1l* mutants at P150. Later, we have verified the hepatic NAD^+ depletion also in much younger (P33-35) *Bcs1l*$^{p.S78G}$ mice and in the mutants on the mtDNA background with the short survival (Fig. 9, unpublished results). Interestingly, the NAD^+ depletion was more pronounced in the juvenile *Bcs1l*$^{p.S78G}$ mice. We also analyzed protein poly-ADP ribosylation and CD38 expression as these may significantly contribute to NAD^+ consumption (**II**, Fig. 1E-G, Supplementary Fig. 2). These were unchanged across the genotypes, which suggest that the decrease in hepatic NAD^+ is mainly due to repressed NAD^+ biosynthesis.

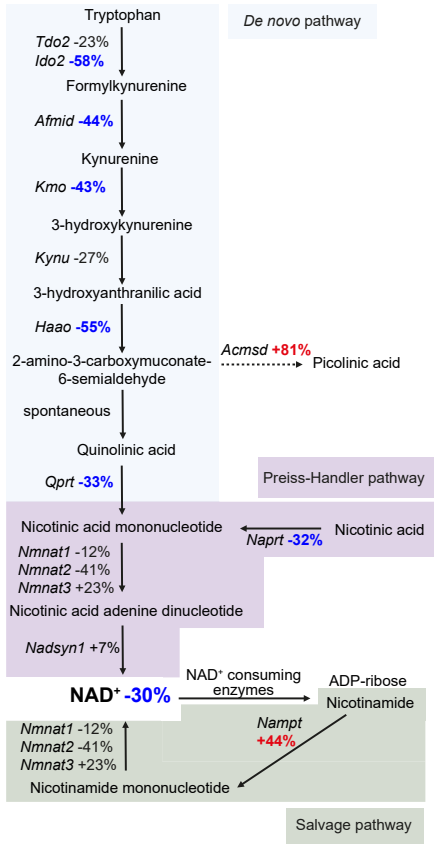

Figure 8. Expression of NAD⁺ biosynthesis-related genes in the liver of *Bcs1l*$^{p.S78G}$ mice. The bolded colors indicate significantly (p<0.05***)*** upregulated (red) or downregulated (blue) genes in *Bcs1l*$^{p.S78G}$ mice at postnatal day 150 (P150) as compared to wild-types (n=5 for wild-types and n=6 for *Bcs1l*$^{p.S78G}$). Average change in NAD⁺ concentration at P150 is also shown.

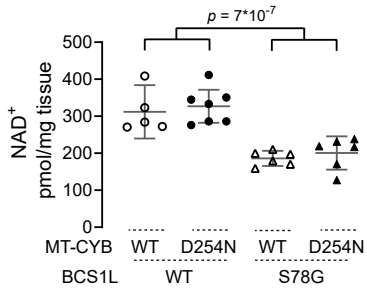

Figure 9. Hepatic NAD⁺ levels in juvenile (P33-35) *Bcs1l*$^{p.S78G}$ mice. The measured samples were from study **IV** F1 hybrid mice with and without the *mt-Cyb*$^{p.D254N}$ variant. The error bars represent 95% confidence interval of the mean. An enzymatic assay with cyclic signal amplification based on alcohol dehydrogenase and a tetrazolium dye reduction was used for the measurements.

9.3.2 NR supplementation does not affect the disease progression

With an aim to correct the NAD^+ depletion, we initiated a randomized controlled intervention with NR supplementation starting at weaning (P21) and lasting for 13 weeks. Behavioral scoring and monitoring of weight loss, performed in blinded fashion, showed no improvement in the condition of the *Bcs1l*$^{p.S78G}$ mice (**II**, Fig. 3A). This was in line with unaltered hepatopathy progression as evaluated by quantification of liver fibrosis, hepatocyte death, ductular reactions, and liver enzyme activities in plasma (**II**, Fig. 3C-G). We also repeated the intervention in *Bcs1l*$^{p.S78G}$ mice on the *mt-Cyb*$^{p.D254N}$ mtDNA background with a more severe disease progression and assessed survival as the main outcome parameter (**II**, Fig. 3H). The survival was unaffected.

9.3.3 NR alters hepatic NAD^+ metabolome but does not correct the NAD^+ depletion

A targeted liver NAD^+-metabolome analysis verified the decreased NAD^+ in *Bcs1l*$^{p.S78G}$ mice (**II**, Fig 2A). However, this was unaffected by NR administration. Neither did NR affect the nicotinamide or ADP-ribose concentrations (**II**, Fig. 2C,H), two metabolites of NAD^+ consuming processes[234]. A clear increase in three degradation metabolites of nicotinamide by NR, nevertheless, suggested that NR increased metabolic fluxes involving nicotinamide (**II**, Fig. 2D-F). NR also increased nicotinic acid adenine dinucleotide (NAAD) concentration (**II**, Fig. C). In light of the most recent understanding of mammalian NAD^+ biosynthetic routes,[190,192] the increased NAAD likely reflects the proportion of NR converted first to nicotinamide then to nicotinic acid by the gut microbiota and then metabolized by the liver via the Preiss-Handler pathway to NAAD. The increase in NAAD concentration also suggests increased biosynthetic flux towards NAD^+.[234] Figure 10 summarizes the NR-induced hepatic NAD^+ metabolome changes in *Bcs1l*$^{p.S78G}$ mice. One reason the NR

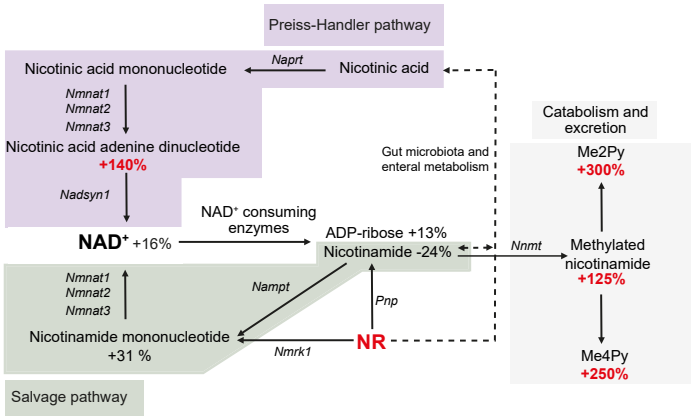

Figure 10. Effect of NR on NAD^+ and related metabolites in the liver of *Bcs1l*$^{p.S78G}$ mice. The bolded red percent values indicate significantly (p<0.05) increased metabolite concentrations (n=5/group).

supplementation did not increase hepatic NAD^+ concentration, at least at the fixed end point, could have been due to the role of liver in maintaining circulating nicotinamide to support NAD^+ biosynthesis in extrahepatic tissues. A recent study on NMN in CI-deficient mice (*Ndufs4* knockout) showed similar refractory NAD^+ depletion in liver, heart and brain but efficient NAD^+ repletion in skeletal muscle.[206]

9.3.4 Mitochondria-related parameters remain unchanged by NR administration

In line with the lack of effect on hepatic NAD^+, NR did not alter mitochondrial respiratory function or mitochondrial mass (**II**, Fig. 4A-C). Furthermore, we performed a label-free quantitative proteomics from liver mitochondria. Out of 572 quantified annotated mitochondrial proteins none were differentially expressed in *Bcs1l*$^{p.S78G}$ mice due to NR administration at false-discovery rate (FDR) of 0.05 (**II**, Supplementary Table 1). As a comparison, the *Bcs1l*$^{p.S78G}$ mutation altered the expression of one quarter of the quantified mitochondrial proteins (fold change >1.4, FDR-adjusted p value < 0.05).

9.3.5 NAD^+-independent regulation of SIRT1 and SIRT3 in *Bcs1l*$^{p.S78G}$ mice

SIRT1 and SIRT3 are the main targets of NAD^+-repletion therapies.[128] These two sirtuin deacetylases respond to alterations in cellular energy state by monitoring NAD^+ levels. The *Bcs1l*$^{p.S78G}$ mice have a profoundly altered energy metabolism involving hypoglycemia, and depletion of glycogen and fat stores (Study **I**, and[18,117,158]). These manifestations were unaffected by NR supplementation (**II**, Fig. 5A-B). Increase in SIRT1 activity due to elevated cellular NAD^+ is only one branch of cellular signals that try to balance energy homeostasis upon nutrient scarcity.[11] Another key regulator is AMPK, which monitors cellular AMP/ATP and ADP/ATP ratios. The regulatory network upstream and downstream of SIRT1 and AMPK are complex and these regulators also regulate each other. Glucose deprivation can activate AMPK independently of changes in adenine nucleotides.[235] Accordingly, we found increased activating phosphorylation of AMPK in the liver of *Bcs1l*$^{p.S78G}$ mice (**II**, Fig. 5C and Supplementary Fig. 5A). Moreover, PKA/cAMP signaling cascade, triggered e.g. by glucagon and adrenergic exposure, stimulates SIRT1 activity and decreases its affinity for NAD^+.[236] Hepatic cAMP levels were increased in *Bcs1l*$^{p.S78G}$ mice (**II**, Fig. 5E). cAMP is also a direct activator of SIRT3.[237] Interestingly, *Bcs1l*$^{p.S78G}$ mice had decreased acetylation of the SIRT3 target protein SOD2 in the liver, suggesting increased SIRT3 activity despite the decreased NAD^+ levels. (**II**, Fig. 5F). In addition, AMPK can increase SIRT1 activity indirectly through the upregulation of the rate-limiting NAMPT in the NAD^+ salvage pathway.[238] *Bcs1l*$^{p.S78G}$ mice showed increased hepatic gene and protein expression of NAMPT (**II,** Fig. 1B, Fig. 5D), but obviously this upregulation was insufficient to maintain normal NAD^+ levels.

A key downstream target of both SIRT1 and AMPK in the regulation of mitochondrial function is PGC-1α.[119] As already seen in study **I**, PGC-1α was upregulated at transcript level in *Bcs1l*$^{p.S78G}$ mice (**II**, Fig. 5G). This upregulation was also present at protein level (**II**, Fig. 5G and Supplementary Fig. 5B). One of the aims of NAD^+ repletion therapies is to

enhance oxidative metabolism including fatty acid oxidation.[129,239] At transcriptome and mitochondrial proteome level the *Bcs1l*$^{p.S78G}$ mice showed repressed *de novo* lipogenesis and upregulated fatty acid oxidation independently of NR (**II**, Fig. 5I-L).

Sirtuins mainly function as lysine deacetylases.[179] Cellular protein acetylation is balanced by acetylation and deacetylation. The acetylation of lysine residues in proteins requires acetyl-CoA, the concentration of which in cytoplasm and nucleus largely depends on the activity of ATP citrate lyase (ACLY).[240] In the liver of *Bcs1l*$^{p.S78G}$ mice, acetyl-CoA concentration was one fourth of that in wild-type mice, and ACLY was downregulated at transcript and protein level (**II**, Fig. 6A-C). The analysis of lysine acetylation in the liver showed no aberrant acetylation in *Bcs1l*$^{p.S78G}$ mice at P115 (**II**, Fig.6 D). However, at P30 in *Bcs1l*$^{p.S78G}$ mice on mt-Cyb$^{p.D254N}$ background the acetylation of some proteins was increased (**II**, Supplementary Fig. 6). Nevertheless, NR administration did not affect global protein acetylation in either mouse cohort.

In summary, many canonical metabolic events associated with SIRT1 and SIRT3 activation in NAD^+-targeting therapies were already upregulated in the *Bcs1l*$^{p.S78G}$ mice and were not further stimulated by NR supplementation.

9.4 Late-onset phenotypes and the effect of AOX (III)

AOXs are non-mammalian mitochondrial terminal oxidases that can facultatively bypass the CIII-CIV segment of the respiratory electron transfer.[212] In conditions of CIII or CIV blockade, AOX-mediated respiration maintains quinol oxidation and electron transfer, albeit with decreased OXPHOS capacity. We crossbred *Bcs1l*$^{p.S78G}$ mice with mice expressing *Ciona intestinalis* alternative oxidase[219] with the aim to alleviate decreased respiratory electron transfer-related metabolic disturbances. In this study, we also characterized the late-onset phenotypes of the *Bcs1l*$^{p.S78G}$ mice. An extensive description of the effect of AOX on *Bcs1l*$^{p.S78G}$ mice is presented in the thesis of Dr. Rajendran.[241] Here, a summary and relevant parts are discussed in relation to the studies **I**, **II** and **IV**.

9.4.1 Chronic liver and kidney disease in *Bcs1l*$^{p.S78G}$ mice

Neonatal liver and kidney disease are the most prominent manifestations of the GRACILE syndrome.[17,95] Similarly, the *Bcs1l*$^{p.S78G}$ mice show early-onset (P24-26) rapidly progressing liver and kidney disease (**I**, **II**, **IV** and[18]). In contrast to the Lund University C57BL/6JBomTac *Bcs1l*$^{p.S78G}$ mice with juvenile lethality (**II**, **IV** and[18,116]), the *Bcs1l*$^{p.S78G}$ mice on C57BL/6JCrl background did survive the early-onset metabolic crisis (**I**, **II**). In the study **III,** we determined their median lifespan to be 210 days (**III**, Fig. 1B). Strikingly, AOX expression extended the median lifespan to 590 days. At the end stage, the *Bcs1l*$^{p.S78G}$ mice, with and without AOX transgene, showed prominent liver and kidney fibrosis, indicating chronic tissue damage (**III**, Fig. 2C, D). The increase in plasma liver enzyme activities was similar or somewhat attenuated in comparison to measurements

from earlier time-points in studies **I** and **II** (Fig. 11A, B), suggesting an on-going damage but eventual stabilization of the liver condition. AOX did not affect these parameters of liver damage at P200. Interestingly, the hepatic *Gdf15* expression, a marker of mitochondrial dysfunction and overall morbidity,[242] was elevated several-fold in young (P30-45) *Bcs1l*$^{p.S78G}$ mice (**I**, **IV**), but at the age of 150 days it was similar as in wild-types (Fig. 11C).

Despite the extension of lifespan of *Bcs1l*$^{p.S78G}$ mutants and verified AOX activity in isolated liver mitochondria (**III**, Fig. 6H), AOX had little effect in the liver on tissue histology (Fig. 2C), mitochondrial morphological aberrations (**III**, Fig. 3C-F), or transcriptome changes (**III**, Fig. 4) in mice older than 150 days, suggesting amelioration of the condition of other tissues. In the kidneys of *Bcs1l*$^{p.S78G}$ mice, AOX clearly had an effect. AOX normalized the kidney atrophy (**III**, Fig. 2A-B), some histological lesions (**III**, Fig. 2C-D and Supplementary Fig. 1), and mitochondrial morphology in proximal tubules (**III**, Fig. 3B-F). However, AOX had minimal effect on albuminuria (**III**, Fig. 2H) and global transcriptome changes (**III**, Fig. 4). In fact, the expression of many highly up-regulated genes due to the *Bcs1l*$^{p.S78G}$ mutation were either unaffected or further induced by AOX (**III**, Fig. 4L). These results suggested that the dramatic extension of lifespan by AOX was not predominantly related to improved kidney function

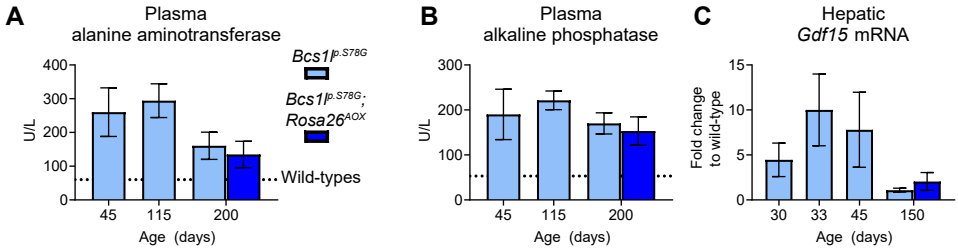

Figure 11. A meta-analysis of plasma liver enzyme activities (**A**-**B**) and hepatic gene expression of *Gdf15* (**C**) from studies **I**-**IV**. The bar graphs and their error bars represent mean value and 2 SDs. The dashed lines represent average values in wild-type mice.

9.4.2 Late-onset lethal cardiomyopathy and its prevention by AOX

Cardiomyopathy has not been reported in patients with *BCS1L* mutations. However, it remains unclear whether those patients who do survive into adulthood will eventually develop a cardiomyopathy. Similarly, we have not observed any indications of cardiomyopathy in young (<P120) *Bcs1l*$^{p.S78G}$ mice (**I**, **II**, **IV**, and[18]). In addition, the CIII deficiency in the juvenile period (<P40) of the mutant mice is less pronounced in the heart (50% of wild-type) in comparison to the liver (20-35% of wild-type) (**IV** and[18]). However, when we collected the end-stage samples (>P190), the immediate observation was a dilating cardiomyopathy and its prevention by AOX (**III**, Fig. 2A). The echocardiography analyses showed failing heart few days before the terminal stage, indicating cardiomyopathy as the cause of the death (**III**, Fig. 2E-F). In contrast, at P150, before the macroscopical or histological alterations, only minimal functional defects in the heart were observable (**III**, Supplementary Fig. S1). CIII activity was 35% of wild-type values (**III**, Fig. 6F), which

compromised OXPHOS (**III**, Fig. 6 I-J). The mitochondrial morphology was also disturbed (**III**, Fig. 3 B-F). In contrast, the heart mitochondria of AOX-expressing *Bcs1l*$^{p.S78G}$ mice had normal ultrastructure (**III**, Fig. 3 B-F) and were able to maintain wild-type respiratory electron transfer (**III**, Fig. 6 I-J). Moreover, AOX caused a global normalization of cardiac transcriptome at P150 (**III**, Fig. 4), a time point when the hearts of *Bcs1l*$^{p.S78G}$ mice were still functionally asymptomatic.

One peculiar effect of AOX on *Bcs1l*$^{p.S78G}$ mice was the increased RISP amount in CIII and improved CIII activity in the heart mitochondria (**III**, Fig. 6A-C, F). Even more peculiar was the totally opposite response in the liver and kidney mitochondria. In study **I**, we also found that ketogenic diet improved the CIII assembly and activity in the liver. Together these results imply that the *Bcs1l*$^{p.S78G}$-related CIII assembly defect is not a static condition but affected by still unknown factors. One potential regulator of BCS1L function, and possibly affected by AOX, is mitochondrial ATP/ADP ratio. In yeast, mutations that decrease the ATP hydrolysis activity of ATP synthase can compensate certain *Bcs1* mutations.[243] At the same time with our study, Dogan et al. studied the effect of AOX on conditional *Cox15* knockout mice with skeletal muscle-specific CIV deficiency.[244] In their model, AOX expression decreased mitochondrial mass, exacerbated IV deficiency, and decreased the lifespan. We did not find any indications of skeletal muscle-related adverse effects (our behavioral scoring and independent phenotype screening by German Mouse Clinic).

In summary, AOX-mediated respiration in a severe CIII deficiency was sufficient to maintain largely normal function of the heart, a tissue that has perhaps the highest requirement for OXPHOS in the body. Importantly, AOX provided a long-term protection from the cardiomyopathy as there was no sign of cardiomyopathy even in those mice that lived past 600 days (**III**, Supplementary Figure EV2).

9.5 A homoplasmic *mt-Cyb* variant exacerbates CIII deficiency in *Bcs1l*$^{p.S78G}$ mice (IV)

During the studies **I**-**III**, we observed an approximately five-fold difference in the lifespan of *Bcs1l*$^{p.S78G}$ mice in two closely related congenic substrains. We found out that the original mouse colony in Lund University, Sweden, had been maintained for years without obtaining new breeding mice from any commercial source. Therefore, we suspected that a genetic drift had taken place in the original mouse colony and proceeded to whole genome sequencing to identify potential *Bcs1l*$^{p.S78G}$-interacting genetic changes.

9.5.1 Identification of a novel mtDNA variant

Whole genome sequencing identified 4449 homozygous single-nucleotide polymorphisms or insertions or deletions differing between the substrains (Lund University C57BL/6JBomTac vs Harlan C57BL/6JCrl). Only eight of these were in the coding-regions

of genes. Of these eight, two were synonymous and five potentially biological relevant changes had no obvious connection to mitochondrial function or energy metabolism (**IV**, Supplementary Table 1). However, one single-nucleotide change of Lund University substrain was in mtDNA (m.G14904A) and not present in any *Mus musculus* sequence in data bases. This variant changes a highly conserved negatively charged residue in MT-CYB (p.D254N), the essential catalytic subunit of CIII (**IV**, Fig. 1A). Moreover, the change is in a region known to interact with RISP, which assembly is compromised in *BCS1L* mutations. Genotyping of old DNA samples from the past generations from the Lund University colony consistently verified the presence of *mt-Cyb*$^{p.D25N4}$ since May 2008 (**IV**, Supplementary Fig. 1A). Interestingly, two early-generation female mice had given progeny carrying both wild-type and variant mtDNA, suggesting initial heteroplasmy. However, no signs of heteroplasmy were detectable in different somatic tissues in later generations (**IV**, Supplementary Fig. 1B). In line with the homoplasmic nature of the variant, the congenic Lund University colony *Bcsl*$^{p.S78G}$ homozygotes show highly consistent lifespan of approximately 1 month (Study **II**, and[116,117])

After finding this obvious candidate gene, we utilized the maternal inheritance of mtDNA and crossbred *Bcs1l*$^{p.S78G}$ heterozygotes to obtain F1 hybrid mice with equal nuclear DNA but differing in their mtDNA (**IV**, Fig 1B). The Lund colony females consistently transmitted the short-survival phenotype to the *Bcs1l*$^{p.S78G}$ homozygotes, but the males did not (**IV**, Fig 1C). As the *mt-Cyb*$^{p.D254N}$ variant was the only difference in the mtDNA between the substrains, this variant is the cause of the survival difference. In line with the decreased survival, *mt-Cyb*$^{p.D254N}$ aggravated the kidney disease and caused massive hepatocyte death at the end stage in *Bcs1l*$^{p.S78G}$ homozygotes (**IV**, Fig. 1G-H Supplementary Fig. 3-4).

9.5.2 *Mt-Cyb*$^{p.D254N}$ decreases CIII activity below survival threshold in *Bcs1l*$^{p.S78G}$ mice

The *Bcs1l*$^{p.S78G}$ homozygotes of Lund University colony show a progressive loss of CIII activity.[18] At birth, the homozygotes have almost normal CIII activity in the liver but at the time of expected spontaneous death it is less than 25% of wild-type values. In the University of Helsinki colony, we have not seen as dramatic loss of CIII activity (study **I** and **III**). The genetically comparable F1 mice allowed us to compare more directly the effect of *mt-Cyb*$^{p.D254N}$ variant. In the liver, kidney, skeletal muscle and heart of *Bcs1l*$^{p.S78G}$ mice, *mt-Cyb*$^{p.D254N}$ caused a further decrease in CIII activity (**IV**, Fig.2, Supplementary Fig. 5). We also measured CIII activity in mice that we had backcrossed onto C57BL/6JCrl background. In these mice also, *mt-Cyb*$^{p.D254N}$ exacerbated the CIII deficiency. The *mt-Cyb*$^{p.D254N}$ did not cause consistently measurable difference in CIII activity in *Bcs1l* wild-type mice in liver, kidney, or skeletal muscle (**IV**, Fig.2, Supplementary Fig. 5). However, three different sample sets showed decreased cardiac CIII activity in *Bcs1l* wild-type mice carrying the *mt-Cyb*$^{p.D254N}$ variant.

9.5.3 Mt-Cyb$^{p.D254N}$ restricts RISP head domain movement

Next, we set out to investigate how the *mt-Cyb$^{p.D254N}$* variant affects CIII function. The MT-CYB is an essential structural core of CIII and the D254N amino acid change is in a region interacting with RISP, therefore we used blue-native gel electrophoresis and Western blot analyses to investigate whether it interferes with RISP assembly into CIII (**IV**, Fig.3). As expected (study **I**, and[18,116]), the liver and kidney mitochondria of *Bcs1l$^{p.S78G}$* mice showed diminished amount of RISP in CIII. However, *mt-Cyb$^{p.D254N}$* variant did not significantly alter CIII amount or assembly.

Because the CIII amount and composition were unaffected, we sought alternative explanations for the synergistic decrease in CIII activity due to *Bcs1l$^{p.S78G}$* and *mt-Cyb$^{p.D254N}$*. Based on the crystal structures of CIII, the RISP head domain brushes the MT-CYB *ef* loop containing the D254N substitution during the electron transfer between the Q_o site and cytochrome c_1 (**IV**, Fig. 5A-C). Molecular dynamics simulation provided a further insight into the interaction between *mt-Cyb$^{p.D254N}$* and RISP. The simulations suggested that the D254N restricts the conformational flexibility of T250-V270 segment in the mt-CYB *ef* loop with simultaneous decrease in the mobility of RISP P136-W146 residues (**IV**, Fig. 5D-G). These results predict that D254N could affect RISP head domain movement during the electron transfer.

To test the computational prediction, we employed a *Rhodobacter capsulatus* model in which the cytochrome b can be mutagenized and the cytochrome bc_1 complex isolated.[245] In this organism, D258N substitution, equivalent to the *Mus musculus* D254N, supported cytochrome bc_1-dependent photosynthetic growth and did not alter the maximal enzymatic activity (**IV**, Supplementary Table 2). The purified cytochrome bc_1 complex from *Rhodobacter capsulatus* allowed the monitoring of RISP head domain movement using pulse electron paramagnetic resonance (EPR) spectroscopy. In this method, the phase relaxation of RISP Fe-S cluster in proximity to oxidized heme b_L of cytochrome *b* gives a signal enhancement that allows the monitoring of RISP head domain distribution between Q_o and cytochrome c_1 positions.[89,245] In native enzyme preparations, the RISP head domains are equally distributed between the two positions.[245] The D258N substitution shifted the RISP head domain positional distribution towards the Q_o site (**IV**, Fig. 5H-I).

In summary, the CIII kinetics disturbance due to *mt-Cyb$^{p.D254N}$* was subtle, but it clearly affected a rate-limiting step in *Bcs1l$^{p.S78G}$* mice with insufficient RISP incorporation into CIII. Moreover, *mt-Cyb$^{p.D254N}$* clearly affected cardiac CIII activity in *Bcs1l* wild-type mice. CIII is inactive without RISP because the first electron-transfer reaction does not occur. However, as CIII is a dimer, it is possible that the *Bcs1l$^{p.S78G}$* mice have heterodimers containing only one RISP. Artificial bacterial cytochrome bc_1 heterodimers with only one active Q_o site have almost wild-type enzyme activity due to the inter-monomer electron transfer via the two closely located b_L hemes.[246,247] Evidence also exits that the CIII dimer may operate under half-of-the-sites reactivity mechanisms in which only one Q_o site operates at any time,[246] a process that might be under physiological regulation.[248] It is tempting to speculate that the *mt-Cyb$^{p.D254N}$* variant might affect a rate-limiting step in heterodimers containing single

RISP or in wild-type cardiac mitochondria in which CIII might harbor posttranslational modifications that modify the CIII processivity.

9.5.4 Metabolic consequences of *mt-Cyb*$^{p.D254N}$ mtDNA background

To assess the effect of *mt-Cyb*$^{p.D254N}$ variant on mitochondrial bioenergetics, we subjected liver and kidney mitochondria to respirometry analysis (**IV**, Fig. 4, Supplementary Fig. 7-9). In line with the exacerbated CIII deficiency, *Bcs1l*$^{p.S78G}$*;mt-Cyb*$^{p.D254N}$ mice showed a further decrease in CI and CII-mediated phosphorylating respiration (**IV**, Fig. 4A). In *Bcs1l* wild-type mice, *mt-Cyb*$^{p.D254N}$ did not affect this parameter. Addition of an ATP-synthase inhibitor to induce high-membrane potential state and leak respiration, however, revealed a *Bcs1l*$^{p.S78G}$-independent decrease in oxygen consumption by *mt-Cyb*$^{p.D254N}$ (**IV**, Fig. 4B). The dissipation of membrane potential abolished this *mt-Cyb*$^{p.D254N}$-related difference in oxygen consumption in *Bcs1l* wild-type mice (**IV**, Fig. 4C). Due to decreased leak respiration, the *Bcs1l* wild-types carrying *mt-Cyb*$^{p.D254N}$ also showed increased electron-transfer coupling efficiency (**IV**, Fig. 4D-E, Supplementary Fig. 7). As CIII is a proton translocase, the reduced leak respiration suggests that *mt-Cyb*$^{p.D254N}$ decreases proton leakage at CIII, or indirectly elsewhere, or affects a rate-limiting step when the enzyme is operating against high membrane potential.

The Q_o site of CIII is one potential source of mitochondrial ROS.[60] However, mutations that cause RISP head domain to predominantly locate to Q_o site, similar to *mt-Cyb*$^{p.D254N}$, tend to decrease superoxide production.[64] In line with this, the D258N substitution in *Rhodobacter capsulatus* did not detectably affect the maximal antimycin-induced superoxide production by the enzyme (**IV**, Supplementary Table 2). Neither did we observe altered hydrogen peroxide emission by isolated state 3 respiring mouse mitochondria with succinate as substrate and reverse-electron flow blocked with rotenone (**IV**, Supplementary Fig. 11). However, these results do not exclude altered ROS production elsewhere in the electron transfer, or differences after induction of high mitochondrial membrane potential.

To assess whether the subtle disturbance in mitochondrial bioenergetics due *mt-Cyb*$^{p.D254N}$ affects whole-body metabolism, we subjected the mice to indirect calorimetry. The *mt-Cyb*$^{p.D254N}$*;Bcs1l*$^{p.S78G}$ mice were clearly a distinct group showing low respiratory exchange ratio implying increased fatty acid oxidation (**IV**, Fig. 6A,B). Their energy expenditure was also decreased (**IV**, Fig. 6C). The daytime measurements did not distinguish the three other genotypes from each other (**IV**, Fig. 6A-C). However, during nighttime, when the mice are most activity, both the *mt-Cyb*$^{p.D254N}$ variant and the *Bcs1l*$^{p.S78G}$ mutation caused a similar decrease in respiratory exchange ratio and energy expenditure in comparison to wild-type mice. Differences in physical activity did not explain the results (**IV**, Supplementary Fig. 14). The unexpectedly large effect of *mt-Cyb*$^{p.D254N}$ on whole-body metabolism in apparently healthy mice led us to measure hepatic gene expression of two well-established markers of mitochondrial dysfunction, *Fgf21* and *Gdf15*.[242] In study **I**, we showed that both of them are upregulated in the liver of *Bcs1l*$^{p.S78G}$ *mice* (**I**, Fig. 4H). The *mt-Cyb*$^{p.D254N}$ variant did not further increase *Fgf21* or *Gdf15* expression in *Bcs1l*$^{p.S78G}$ mutants (**IV**, Fig. 6D,E).

However, surprisingly, the *mt-Cyb*$^{p.D254N}$ variant on its own induced *Fgf21* expression to a similar degree as the pathogenic *Bcs1l*$^{p.S78G}$ mutation (**IV**, Fig. 6D). In normal physiology, FGF21 is mainly a hepatocyte-derived stress-inducible paracrine and endocrine factor regulating energy metabolism.[153] In mitochondrial dysfunction, mitochondrial integrated stress response induces *FGF21* expression in the affected tissues.[249] Figure 12 summarizes the identified effects of *mt-Cyb*$^{p.D254N}$ variant.

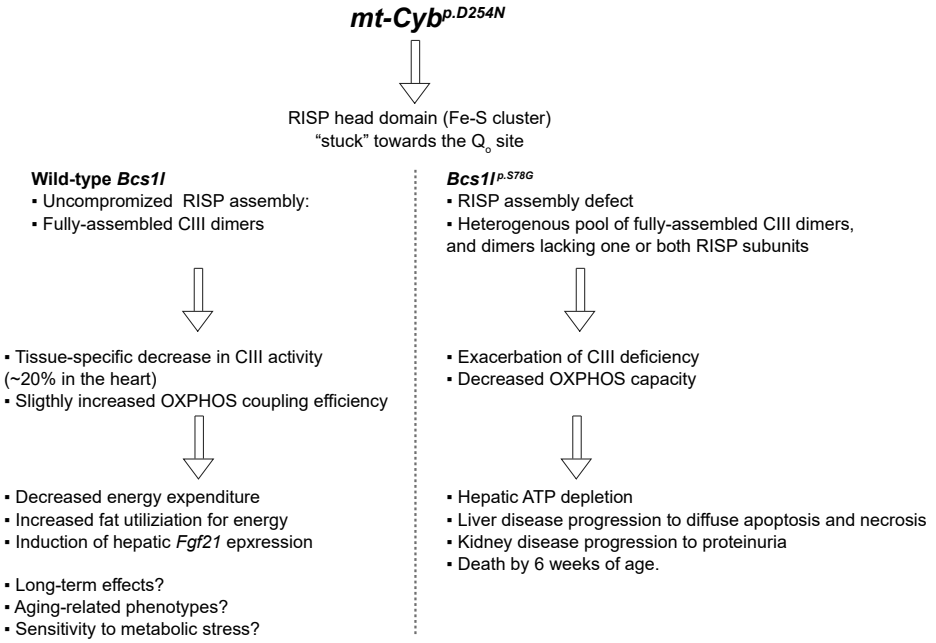

Figure 12. Summary of effects of *mt-Cyb*$^{p.D254N}$ variant on *Bcs1l* wild-type and mutant mice.

10 CONCLUSIONS AND FUTURE PROSPECTS

CIII deficiencies are still scarcely studied among the mitochondrial diseases. This thesis project has extended the characterization of CIII-related disease mechanisms and investigated two proposed therapies in a mouse model of GRACILE syndrome. Moreover, we identified a novel homoplasmic mtDNA variant that can be utilized to study subtle CIII dysfunction or to exacerbate CIII deficiency in *Bcs1l*$^{p.S78G}$ mice and possibly in other mouse models of CIII deficiency.

*Study **I***

In study **I**, we showed that ketogenic diet can ameliorate a CIII deficiency-related hepatopathy in mice. Some studies have proposed that ketogenic diet increases mitochondrial biogenesis.[162,167] Our results did not support this theory. Despite this, ketogenic diet clearly improved mitochondrial function and morphology in *Bcs1l*$^{p.S78G}$ mice. The mechanism of action of ketogenic diet, however, remains elusive. A dramatic shift in energy metabolism follows the extreme carbohydrate-restriction and high fat content of the ketogenic diet. Therefore, it is evident that ketogenic diet necessarily modulates mitochondrial function. However, which of the metabolic adaptations to ketogenic diet are beneficial and which perhaps harmful in mitochondrial disorders requires further studies. Moreover, ketogenic diet may mediate its effects via the ketone body β-hydroxybutyrate, which is now a well-recognized signaling molecule.[250] Our transcriptomic data suggested that ketogenic diet affected macrophage polarization in the *Bcs1l*$^{p.S78G}$ mice. A recent study showed that stimulation of HCAR2 receptor with β-hydroxybutyrate attenuates acute liver damage via altered macrophage polarization.[233] In addition, β-hydroxybutyrate modulates macrophage polarization via inhibition of NLRP3 inflammasome.[175] β-hydroxybutyrate is also a direct substrate for histone β-hydroxybutyrylation[251]. The signaling functions of ketone bodies in *Bcs1l*$^{p.S78G}$ mice, without the metabolic adaptations related to carbohydrate restriction and high fat content, could be studied with ketone ester supplementation[252].

*Study **II***

NAD^+-repletion therapies have proven beneficial in a number of preclinical models of various disease conditions.[128] Yet, the knowledge on NAD^+ repletion in different tissues in primary mitochondrial diseases is still very limited. We were the first to study NAD^+ repletion in isolated CIII deficiency and in a mitochondrial hepatopathy. In contrast to mitochondrial myopathy models,[130,131] the hepatic NAD^+ depletion and the hepatopathy of *Bcs1l*$^{p.S78G}$ mice were refractory to the NAD^+ precursor NR. Considering the fact that the tryptophan is a major precursor for hepatic NAD^+ biosynthesis,[192] and this pathway being repressed in *Bcs1l*$^{p.S78G}$ mice, an alternative NAD^+ repletion strategy such as the inhibition of ACMSD to maximize tryptophan utilization for NAD^+ biosynthesis,[205] could have proven more effective than NR. Nonetheless, the investigation of the downstream effects of NAD^+ depletion and the linked cellular signaling events suggested that the starvation-like metabolic state of *Bcs1l*$^{p.S78G}$ mice endogenously stimulates the very same metabolic adaptations that are the primary targets of NAD^+-repletion therapies.

We did not analyze in detail the effects of NR on other tissues than liver due to the lack of improvement in the general condition of *Bcs1l*$^{p.S78G}$ mice. Despite this, taking into the consideration the role of liver in maintaining circulating nicotinamide for NAD^+ biosynthesis in extrahepatic tissues, it is possible that NR administration increased NAD^+ concentrations in other tissues such as in skeletal muscle.

*Study **III***

AOXs are intriguing respiratory enzymes that most animals have lost during evolution.[253] They function as quinol overflow valves to alleviate an insufficiency of the CIII-CIV segment of the electron transfer. Our results showed that, when introduced into the CIII-deficient mice, AOX restored respiratory electron transfer in the heart. This was sufficient to give long-term protection from cardiomyopathy and allow near-normal lifespan. Our results are consistent with the heart failure of *Bcs1l*$^{p.S78G}$ mice being due to a primary mitochondrial cardiomyopathy, but it is also highly likely that the liver and kidney disease contribute to the cardiomyopathy progression. Especially, the effect of AOX on kidney morphology is interesting despite that it did normalize the function of this organ. Unexpectedly, at the end-stage, AOX had only minimal effect on the liver, the most affected organ in the GRACILE syndrome. It appears that the CIII deficiency was not severe enough in the liver of relatively old *Bcs1l*$^{p.S78G}$ mice to allow AOX-mediated respiration *in vivo*. Whether AOX affects the metabolic crisis of the juvenile period involving a more severe hepatic CIII deficiency and whether the AOX can rescue the early lethality in *Bcs1l*$^{p.S78G}$*;mt-Cyb*$^{p.D254N}$ mice are ongoing projects in our laboratory. We are also utilizing AOX to study in more detail mitochondrial ROS signaling and the consequences of coenzyme Q pool overreduction in *Bcs1l*$^{p.S78G}$ mice.

*Study **IV***

A stunning 5-fold difference in the lifespan of *Bcs1l*$^{p.S78G}$ mice in two closely related congenic substrains in two animal facilities puzzled us during the studies **I**-**III**. The difference was beyond explanation by any environmental differences between the two animal facilities. Never would we have expected that the underlying genetic difference turned out to be a single-nucleotide change in the only CIII subunit gene in mtDNA, *mt-Cyb*. Even more astonishing was the location of the consequent amino acid change in a segment of MT-CYB *ef* loop interacting with RISP, which incorporation into CIII is compromised by *Bcs1l* mutations.

We demonstrated that the *mt-Cyb*$^{p.D254N}$ variant causes a subtle restriction in the RISP head domain movement. The effects of *mt-Cyb*$^{p.D254N}$ and *Bcs1l*$^{p.S78G}$ on CIII activity were not entirely additive but synergistic. *Bcs1l*$^{p.S78G}$ affects CIII activity indirectly by decreasing the efficacy of RISP insertion into the complex. The small number of fully assembled CIII dimers in *Bcs1l*$^{p.S78G}$ mutants should have a native structure. However, it is possible that most of the RISP in *Bcs1l*$^{p.S78G}$ mutants is in heterodimers containing only one RISP. In

theory and according to bacterial heterodimer models,[246,247] a single-RISP CIII dimer could be enzymatically active and have increased sensitivity to the *mt-Cyb*$^{p.D254N}$ variant. However, investigation of heterodimers and inter-monomer electron transfer was beyond the scope of study **IV**.

No genetic tools exist to introduce targeted mutations into the multicopy mammalian mtDNA. Therefore, the spontaneous homoplasmic *mt-Cyb*$^{p.D254N}$ variant mouse line may prove a highly valuable tool. The *mt-Cyb*$^{p.D254N}$ variant is not overtly pathogenic but neither silent. It consistently decreased cardiac CIII activity in *Bcs1l* wild-type mice. Moreover, in liver and kidney mitochondria, it decreased leak respiration and increased electron transfer coupling efficiency. At whole-body level, *mt-Cyb*$^{p.D254N}$ decreased energy expenditure and most astonishingly, it induced similar hepatic *Fgf21* expression as the pathogenic *Bcs1l*$^{p.S78G}$ mutation. According to the sequence databases, *mt-Cyb*$^{p.D254N}$ is present in three-toed sloths (*Bradypus torquatus*) of South America which have slow metabolism and extremely energy-poor diet.[254] The existence of *mt-Cyb*$^{p.D254N}$ in nature suggests that it might even be beneficial under certain circumstances.

We investigated the effect of *mt-Cyb*$^{p.D254N}$ on ROS production relatively superficially in study **IV**. Our data from mouse and *Rhodobacter capsulatus* model, and also previous studies on similar mutations,[245] indicate that *mt-Cyb*$^{p.D254N}$ does not promote superoxide production at Q_o site. However, *in vivo*, mitochondrial membrane potential and coenzyme Q pool redox status affect ROS production.[65] *Mt-Cyb*$^{p.D254N}$ potentially, as respirometry data indirectly suggests, affects both parameters. A topic of future studies is also the effect of the subtle *mt-Cyb*$^{p.D254N}$-mediated disturbance in mitochondrial bioenergetics and whole-body metabolism on aging or physiology under stressed conditions.

11 ACKNOWLEDGMENTS

This study was carried out at the Folkhälsan Research Center. I thank the Folkhälsan Research Center and the Samfundet Folkhälsan organizations for the excellent facilities, infrastructure, and administration to conduct research. I thank the Doctoral Program in Biomedicine, Faculty of Medicine, University of Helsinki for the opportunity to carry out my doctoral studies.

Samfundet Folkhälsan, Academy of Finland, Swedish Research Council, Finnish Physicians' Society (Finska Läkaresällskapet), Foundation for Pediatric Research in Finland (Lastentautien tutkimussäätiö) and Magnus Ehrnrooth Foundation funded our research group. In addition, Chancellor's travel grants, Biomedicum Helsinki Foundation, and Alfred Kordelin Foundation financially supported my doctoral studies.

I am the most grateful for having had the privilege to develop into a researcher under the supervision and mentoring of Prof. Vineta Fellman and Docent Jukka Kallijärvi. I could not have imagined a more suitable laboratory to encounter the inspiring challenges, to experiment, and to learn all the necessary skills. Vineta, I truly admire your enormous experience and knowledge, genuine interest in our work, and all the work you have done to keep the GRACILE research well-funded and going forward. Jukka, you first taught me the basic skills in the laboratory and introduced me into the field of mitochondria in a way that motivated me to pursue a career as a researcher. I am thankful for the numerous, essentially daily, inspiring discussions we have. These discussions have been scientifically fruitful, but they also have helped me to grow in many ways. I hope we can continue unraveling the mysteries of CIII deficiency.

I warmly thank Prof. Michael Murphy for serving as an opponent and Prof. Elina Ikonen for servings as a custos. This thesis was polished by excellent pre-examination by Docent Eric Dufour and Dr. Cristopher Carroll. I thank my thesis committee members Prof. Vesa Olkkonen and Docent Risto Lapatto for the annual meetings and your motivating feedback.

I thank all the co-authors and collaborators for their important contribution. I am especially thankful to Dr. Matthias Mörgelin for electron microscopy analyses, to Prof. Juha Kere and Dr. Shintaro Katayama for collaboration in transcriptomics in study **I**, to Docent Matti Jauhiainen for lipid analyses and inspiring meetings, to Docent Eija Pirinen for ideas and helping to shape the NR manuscript, to Docent Maciej Lalowski and Dr. Rabah Soliymani for the mitochondrial proteomics (we will eventually publish the entire data…), to Docent Petri Auvinen and Dr. Olli-Pekka Smolander for transcriptomics in study **III**, and to Prof. Howard Jacobs and Dr. Marten Szibor for discussions on AOX. The fluent and outstanding collaboration enabled the unraveling of the details of *mt-Cyb*$^{p.D254N}$ to almost atomic level. My deepest gratitude goes to Prof. Mårten Wikström for the crucial discussions on CIII, to Katarina Truvé for the WGS analysis, to Dr. Vivek Sharma and M.Sci Noora Aho for the molecular dynamics simulations, and to Prof. Artur Osyczka and Dr. Robert Ekiert and their colleagues for the *Rhodobackter capsulatus* work.

I thank all the present and former GRACILE group members. My fellow PhD student, now successfully a doctor, Jayasimman Rajendran, I warmly remember your humble easy-

going attitude even during the most hectic times. You carried a huge responsibility on the animal work and our group's largest project at the time, the AOX study. My warmest gratitude to all your input. Elisa Alppila kept genotyping and other routine work in the lab rolling, which was essential. I gave you many technically demanding protocols, which kept changing all the time, to perform. I am grateful for having had your help. Rishi Banerjee and Vilma Wanne, the newcomers of our group, I am glad to have been able to trust some experiments to you while writing this book. I gratefully appreciate Vladislav Grigorjev's contribution in the initial stages of the *mt-Cyb*$^{p.D254N}$ study and Kristiina Uusi-Rauva's input in the ketogenic diet study. Many thanks to Saara Tegelberg for taking care of the animal work in Lund. I also appreciate your exceptional memory in locating ancient antibodies and other reagents at Folkhälsan.

Numerous people have helped me along the years. My warmest appreciation goes to Dr. Eskil Elmer for taking me into his laboratory to learn mitochondrial respirometry under the excellent guidance from Dr. Sarah Piel and Eleanor Frostner. To Prof. Eero Mervala and Nada Bechavara-Hirvonen for allowing me to use their respirometer, and to Nada for the initial help regarding the respirometry. To Prof. Hannu Sariola, Docent Jouko Lohi and Prof. Hannu Jalanko for guidance in histopathology. To Folkhälsan Research center administration and laboratory management: especially to Ann-liz Träskelin and Teija Toivonen for all the reagent and instrument orders and taking into consideration my wishes. Finally, to Vilma-Lotta Lehtokari for introducing me to Folkhälsan Research Center and to dachshunds (Harmi, Oikku, Metku and Kiusa).

I thank all the family members and friends for understanding my occasional disappearance into the world of science. I apologize for my periods of absence.

12 REFERENCES

1. Martijn J, Vosseberg J, Guy L, Offre P, Ettema TJG. Deep mitochondrial origin outside the sampled alphaproteobacteria. Nature 2018;557:101–5.

2. Imachi H, Nobu MK, Nakahara N, et al. Isolation of an archaeon at the prokaryote–eukaryote interface. Nature 2020;577:519–25.

3. Roger AJ, Muñoz-Gómez SA, Kamikawa R. The origin and diversification of mitochondria. Curr Biol 2017;27:R1177–92.

4. Krebs HA, Johnson WA. The role of citric acid in intermediate metabolism in animal tissues. Enzymologia 1937;4:148–56.

5. Mitchell P. Coupling of phosphorylation to electron and hydrogen transfer by a chemi-osmotic type of mechanism. Nature 1961;191:144–8.

6. Ernster L, Schatz G. Mitochondria: a historical review. J Cell Biol 1981;91:227s–55s.

7. Spinelli JB, Haigis MC. The multifaceted contributions of mitochondria to cellular metabolism. Nat Cell Biol 2018;20:745–54.

8. Calvo SE, Mootha VK. The mitochondrial proteome and human disease. Annu Rev Genomics Hum Genet 2010;11:25–44.

9. Craven L, Alston CL, Taylor RW, Turnbull DM. Recent advances in mitochondrial disease. Annu Rev Genomics Hum Genet 2017;18:257–75.

10. Thorburn DR. Mitochondrial disorders: Prevalence, myths and advances. J Inherit Metab Dis 27:349–62.

11. Whitaker RM, Corum D, Beeson CC, Schnellmann RG. Mitochondrial biogenesis as a pharmacological target: a new approach to acute and chronic diseases. Annu Rev Pharmacol Toxicol 2016;56:229–49.

12. Crofts AR. The cytochrome bc1 complex: function in the context of structure. Annu Rev Physiol 2004;66:689–733.

13. Meunier B, Fisher N, Ransac S, Mazat J-P, Brasseur G. Respiratory complex III dysfunction in humans and the use of yeast as a model organism to study mitochondrial myopathy and associated diseases. Biochim Biophys Acta BBA - Bioenerg 2013;1827:1346–61.

14. Wagener N, Neupert W. Bcs1, a AAA protein of the mitochondria with a role in the biogenesis of the respiratory chain. J Struct Biol 2012;179:121–5.

15. Visapää I, Fellman V, Vesa J, et al. GRACILE syndrome, a lethal metabolic disorder with iron overload, is caused by a point mutation in BCS1L. Am J Hum Genet 2002;71:863–

76.

16. Kotarsky H, Karikoski R, Mörgelin M, et al. Characterization of complex III deficiency and liver dysfunction in GRACILE syndrome caused by a BCS1L mutation. Mitochondrion 2010;10:497–509.

17. Fellman V, Rapola J, Pihko H, Varilo T, Raivio KO. Iron-overload disease in infants involving fetal growth retardation, lactic acidosis, liver haemosiderosis, and aminoaciduria. The Lancet 1998;351:490–3.

18. Levéen P, Kotarsky H, Mörgelin M, Karikoski R, Elmér E, Fellman V. The GRACILE mutation introduced into Bcs1l causes postnatal complex III deficiency: A viable mouse model for mitochondrial hepatopathy. Hepatology 2011;53:437–47.

19. Pernas L, Scorrano L. Mito-morphosis: mitochondrial fusion, fission, and cristae remodeling as key mediators of cellular function. Annu Rev Physiol 2016;78:505–31.

20. Kühlbrandt W. Structure and function of mitochondrial membrane protein complexes. BMC Biol 2015;13:89.

21. Wai T, Langer T. Mitochondrial dynamics and metabolic regulation. Trends Endocrinol Metab 2016;27:105–17.

22. Gustafsson CM, Falkenberg M, Larsson N-G. Maintenance and expression of mammalian mitochondrial DNA. Annu Rev Biochem 2016;85:133–60.

23. Martínez-Reyes I, Chandel NS. Mitochondrial TCA cycle metabolites control physiology and disease. Nat Commun 2020;11:102.

24. Mitchell P, Moyle J. Stoichiometry of proton translocation through the respiratory chain and adenosine triphosphatase systems of rat liver mitochondria. Nature 1965;208:147–51.

25. Frerman FE. Acyl-CoA dehydrogenases, electron transfer flavoprotein and electron transfer flavoprotein dehydrogenase. Biochem Soc Trans 1988;16(3):416–8.

26. Watmough NJ, Frerman FE. The electron transfer flavoprotein: Ubiquinone oxidoreductases. Biochim Biophys Acta BBA - Bioenerg 2010;1797:1910–6.

27. Perales-Clemente E, Bayona-Bafaluy MP, Pérez-Martos A, Barrientos A, Fernández-Silva P, Enriquez JA. Restoration of electron transport without proton pumping in mammalian mitochondria. Proc Natl Acad Sci 2008;105:18735–9.

28. Löffler M, Jöckel J, Schuster G. Dihydroorotat-ubiquinone oxidoreductase links mitochondria in the biosynthesis of pyrimidine nucleotides. Mol Cell Biochem 1997;174:125–9.

29. Luna-Sánchez M, Hidalgo-Gutiérrez A, Hildebrandt TM, et al. CoQ deficiency causes disruption of mitochondrial sulfide oxidation, a new pathomechanism associated with this syndrome. EMBO Mol Med 2017;9:78–95.

30. Hancock CN, Liu W, Alvord WG, Phang JM. Co-regulation of mitochondrial respiration by proline dehydrogenase/oxidase and succinate. Amino Acids 2016;48:859–72.

31. Barrett MC, Dawson AP. Essentiality of ubiquinone for choline oxidation in rat liver mitochondria. Biochem J 1975;148:595–7.

32. Mráček T, Drahota Z, Houštěk J. The function and the role of the mitochondrial glycerol-3-phosphate dehydrogenase in mammalian tissues. Biochim Biophys Acta BBA - Bioenerg 2013;1827:401–10.

33. Cohen HJ, Betcher-Lange S, Kessler DL, Rajagopalan KV. Hepatic Sulfite Oxidase congruency in mitochondria of prosthetic groups and activity. J Biol Chem 1972;247:7759–66.

34. Farrell SR, Thorpe C. Augmenter of liver regeneration: a flavin-dependent sulfhydryl oxidase with cytochrome c reductase activity. Biochemistry 2005;44:1532–41.

35. Goodman RP, Calvo SE, Mootha VK. Spatiotemporal compartmentalization of hepatic NADH and NADPH metabolism. J Biol Chem 2018;293:7508–16.

36. Kubota Y, Nomura K, Katoh Y, Yamashita R, Kaneko K, Furuyama K. Novel mechanisms for heme-dependent degradation of ALAS1 protein as a component of negative feedback regulation of heme biosynthesis. J Biol Chem 2016;291:20516–29.

37. Lill R. Function and biogenesis of iron–sulphur proteins. Nature 2009;460:831–8.

38. Nijhout HF, Reed MC, Lam S-L, Shane B, Gregory JF, Ulrich CM. In silico experimentation with a model of hepatic mitochondrial folate metabolism. Theor Biol Med Model 2006;3:40.

39. Munro D, Baldy C, Pamenter ME, Treberg JR. The exceptional longevity of the naked mole-rat may be explained by mitochondrial antioxidant defenses. Aging Cell 2019;18:e12916.

40. Munro D, Pamenter ME. Comparative studies of mitochondrial reactive oxygen species in animal longevity: Technical pitfalls and possibilities. Aging Cell 2019;18:e13009.

41. Sies H, Jones DP. Reactive oxygen species (ROS) as pleiotropic physiological signalling agents. Nat Rev Mol Cell Biol 2020;21:363-383.

42. Herzig S, Shaw RJ. AMPK: guardian of metabolism and mitochondrial homeostasis. Nat Rev Mol Cell Biol 2018;19:121–35.

43. Kluck RM, Bossy-Wetzel E, Green DR, Newmeyer DD. The release of cytochrome c from mitochondria: a primary site for Bcl-2 regulation of apoptosis. Science 1997;275:1132–6.

44. Osyczka A, Moser CC, Dutton PL. Fixing the Q cycle. Trends Biochem Sci 2005;30:176–82.

45. Smith PM, Fox JL, Winge DR. Reprint of: Biogenesis of the cytochrome bc1 complex and role of assembly factors. Biochim Biophys Acta BBA - Bioenerg 2012;1817:872–82.

46. Zong S, Gu J, Liu T, Guo R, Wu M, Yang M. UQCRFS1N assembles mitochondrial respiratory complex-III into an asymmetric 21-subunit dimer. Protein Cell 2018;9:586–91.

47. Stephan K, Ott M. Timing of dimerization of the bc1 complex during mitochondrial respiratory chain assembly. Biochim Biophys Acta BBA - Bioenerg 2020;1861:148177.

48. Maio N, Kim KS, Singh A, Rouault TA. A single adaptable cochaperone-scaffold complex delivers nascent iron-sulfur clusters to mammalian respiratory chain complexes I–III. Cell Metab 2017;25:945-953.e6.

49. Wagener N, Ackermann M, Funes S, Neupert W. A pathway of protein translocation in mitochondria mediated by the AAA-ATPase Bcs1. Mol Cell 2011;44:191–202.

50. Fölsch H, Guiard B, Neupert W, Stuart RA. Internal targeting signal of the BCS1 protein: a novel mechanism of import into mitochondria. EMBO J 1996;15:479–87.

51. Kater L, Wagener N, Berninghausen O, Becker T, Neupert W, Beckmann R. Structure of the Bcs1 AAA-ATPase suggests an airlock-like translocation mechanism for folded proteins. Nat Struct Mol Biol 2020;27:142–9.

52. Tang WK, Borgnia MJ, Hsu AL, et al. Structures of AAA protein translocase Bcs1 suggest translocation mechanism of a folded protein. Nat Struct Mol Biol 2020;27:202–9.

53. Yedidi RS, Wendler P, Enenkel C. AAA-ATPases in protein degradation. Front Mol Biosci 2017;4:42.

54. Brandt U, Yu L, Yu CA, Trumpower BL. The mitochondrial targeting presequence of the Rieske iron-sulfur protein is processed in a single step after insertion into the cytochrome bc1 complex in mammals and retained as a subunit in the complex. J Biol Chem 1993;268:8387–90.

55. Bottani E, Cerutti R, Harbour ME, et al. TTC19 plays a husbandry role on UQCRFS1 turnover in the biogenesis of mitochondrial respiratory complex III. Mol Cell 2017;67:96-105.e4.

56. Deng K, Shenoy SK, Tso S-C, Yu L, Yu C-A. Reconstitution of mitochondrial processing peptidase from the core proteins (subunits I and II) of bovine heart mitochondrial cytochrome bc 1 complex. J Biol Chem 2001;276:6499–505.

57. Lobo-Jarne T, Ugalde C. Respiratory chain supercomplexes: Structures, function and biogenesis. Semin Cell Dev Biol 2018;76:179–90.

58. Milenkovic D, Blaza JN, Larsson N-G, Hirst J. The enigma of the respiratory chain supercomplex. Cell Metab 2017;25:765–76.

59. Wang Y, Palmfeldt J, Gregersen N, et al. Mitochondrial fatty acid oxidation and the electron transport chain comprise a multifunctional mitochondrial protein complex. J Biol Chem 2019;294:12380–91.

60. Bleier L, Dröse S. Superoxide generation by complex III: From mechanistic rationales to functional consequences. Biochim Biophys Acta BBA - Bioenerg 2013;1827:1320–31.

61. Cape JL, Bowman MK, Kramer DM. A semiquinone intermediate generated at the Qo site of the cytochrome bc1 complex: Importance for the Q-cycle and superoxide production. Proc Natl Acad Sci 2007;104:7887–92.

62. Dröse S, Brandt U. The mechanism of mitochondrial superoxide production by the cytochrome bc1 complex. J Biol Chem 2008;283:21649–54.

63. Rottenberg H, Covian R, Trumpower BL. Membrane potential greatly enhances superoxide generation by the cytochrome bc1 complex reconstituted into phospholipid vesicles. J Biol Chem 2009;284:19203–10.

64. Borek A, Sarewicz M, Osyczka A. Movement of the iron–sulfur head domain of cytochrome bc1 transiently opens the catalytic Qo site for reaction with oxygen. Biochemistry 2008;47:12365–70.

65. Robb EL, Hall AR, Prime TA, et al. Control of mitochondrial superoxide production by reverse electron transport at complex I. J Biol Chem 2018;293:9869–79.

66. Floros VI, Pyle A, Dietmann S, et al. Segregation of mitochondrial DNA heteroplasmy through a developmental genetic bottleneck in human embryos. Nat Cell Biol 2018;20:144–51.

67. Haut S, Brivet M, Touati G, et al. A deletion in the human QP-C gene causes a complex III deficiency resulting in hypoglycaemia and lactic acidosis. Hum Genet 2003;113:118–22.

68. Barel O, Shorer Z, Flusser H, et al. Mitochondrial complex III deficiency associated with a homozygous mutation in UQCRQ. Am J Hum Genet 2008;82:1211–6.

69. Miyake N, Yano S, Sakai C, et al. Mitochondrial complex III deficiency caused by a homozygous UQCRC2 mutation presenting with neonatal-onset recurrent metabolic decompensation. Hum Mutat 2013;34:446–52.

70. Invernizzi F, Tigano M, Dallabona C, et al. A homozygous mutation in LYRM7/MZM1L associated with early onset encephalopathy, lactic acidosis, and severe reduction of mitochondrial complex III activity. Hum Mutat 2013;34:1619–22.

71. Tucker EJ, Wanschers BFJ, Szklarczyk R, et al. Mutations in the UQCC1-interacting protein, UQCC2, cause human complex III deficiency associated with perturbed cytochrome b protein expression. PLoS Genet 2013;9:e1004034.

72. Wanschers BFJ, Szklarczyk R, van den Brand MAM, et al. A mutation in the human CBP4 ortholog UQCC3 impairs complex III assembly, activity and cytochrome b stability. Hum Mol Genet 2014;23:6356–65.

73. Ghezzi D, Arzuffi P, Zordan M, et al. Mutations in TTC19 cause mitochondrial complex III deficiency and neurological impairment in humans and flies. Nat Genet 2011;43:259–63.

74. Gusic M, Schottmann G, Feichtinger RG, et al. Bi-allelic UQCRFS1 variants are associated with mitochondrial complex III deficiency, cardiomyopathy, and alopecia totalis. Am J Hum Genet 2020;106:102–11.

75. Gaignard P, Menezes M, Schiff M, et al. Mutations in CYC1, encoding cytochrome c1 subunit of respiratory chain complex III, cause insulin-responsive hyperglycemia. Am J Hum Genet 2013;93:384–9.

76. Andreu AL, Hanna MG, Reichmann H, et al. Exercise intolerance due to mutations in the cytochrome b gene of mitochondrial DNA. N Engl J Med 1999;341:1037–44.

77. Hinson JT, Fantin VR, Schönberger J, et al. Missense mutations in the BCS1L gene as a cause of the Björnstad syndrome. N Engl J Med 2007;356:809–19.

78. Tobe SS, Linacre A. DNA typing in wildlife crime: recent developments in species identification. Forensic Sci Med Pathol 2010;6:195–206.

79. Ruiz-Pesini E, Lott MT, Procaccio V, et al. An enhanced MITOMAP with a global mtDNA mutational phylogeny. Nucleic Acids Res 2007;35:D823–8.

80. Dumoulin R, Sagnol I, Ferlin T, Bozon D, Stepien G, Mousson B. A novel gly290asp mitochondrial cytochromebmutation linked to a complex III deficiency in progressive exercise intolerance. Mol Cell Probes 1996;10:389–91.

81. Andreu AL, Bruno C, Shanske S, et al. Missense mutation in the mtDNA cytochrome b gene in a patient with myopathy. Neurology 1998;51:1444–7.

82. Valnot I, Kassis J, Chretien D, et al. A mitochondrial cytochrome b mutation but no mutations of nuclearly encoded subunits in ubiquinol cytochrome c reductase (complex III) deficiency. Hum Genet 1999;104:460–6.

83. Keightley JA, Anitori R, Burton MD, Quan F, Buist NRM, Kennaway NG. Mitochondrial encephalomyopathy and complex III deficiency associated with a stop-codon mutation in the cytochrome b gene. Am J Hum Genet 2000;67:1400–10.

84. Wibrand F, Ravn K, Schwartz M, Rosenberg T, Horn N, Vissing J. Multisystem disorder associated with a missense mutation in the mitochondrial cytochrome b gene. Ann Neurol 2001;50:540–3.

85. Emmanuele V, Sotiriou E, Rios PG, et al. A novel mutation in the mitochondrial DNA cytochrome b gene (MTCYB) in a patient with mitochondrial encephalomyopathy, lactic acidosis, and strokelike episodes syndrome. J Child Neurol 2013;28:236–42.

86. Fragaki K, Procaccio V, Bannwarth S, et al. A neonatal polyvisceral failure linked to a de novo homoplasmic mutation in the mitochondrially encoded cytochrome b gene. Mitochondrion 2009;9:346–52.

87. Gil Borlado MC, Moreno Lastres D, Gonzalez Hoyuela M, et al. Impact of the mitochondrial genetic background in complex III deficiency. PloS One 2010;5: e12801.

88. Fisher N, Meunier B. Effects of mutations in mitochondrial cytochrome b in yeast and man. Eur J Biochem 2001;268:1155–62.

89. Ekiert R, Borek A, Kuleta P, Czernek J, Osyczka A. Mitochondrial disease-related mutations at the cytochrome b-iron-sulfur protein (ISP) interface: Molecular effects on the large-scale motion of ISP and superoxide generation studied in Rhodobacter capsulatus cytochrome bc1. Biochim Biophys Acta 2016;1857:1102–10.

90. Song Z, Laleve A, Vallières C, McGeehan JE, Lloyd RE, Meunier B. Human mitochondrial cytochrome b variants studied in yeast: not all are silent polymorphisms. Hum Mutat 2016;37:933–41.

91. Fernández-Vizarra E, Zeviani M. Nuclear gene mutations as the cause of mitochondrial complex III deficiency. Front Genet 2015;6:134.

92. Al-Owain M, Colak D, Albakheet A, et al. Clinical and biochemical features associated with BCS1L mutation. J Inherit Metab Dis 2013;36:813–20.

93. Tegelberg S, Tomašić N, Kallijärvi J, et al. Respiratory chain complex III deficiency due to mutated BCS1L: a novel phenotype with encephalomyopathy, partially phenocopied in a Bcs1l mutant mouse model. Orphanet J Rare Dis 2017;12:73.

94. GRACILE-oireyhtymä - vastasyntyneen vakava mitokondriotauti. Duodecim 2015;128:1560–7.

95. Rapola J, Heikkilä P, Fellman V. Pathology of lethal fetal growth retardation syndrome with aminoaciduria, iron overload, and lactic acidosis (GRACILE). Pediatr Pathol Mol Med 2002;21:183–93.

96. Lonlay P de, Valnot I, Barrientos A, et al. A mutant mitochondrial respiratory chain assembly protein causes complex III deficiency in patients with tubulopathy, encephalopathy and liver failure. Nat Genet 2001;29:57–60.

97. Lynn AM, King RI, Mackay RJ, Florkowski CM, Wilson CJ. BCS1L gene mutation presenting with GRACILE-like syndrome and complex III deficiency. Ann Clin Biochem 2012;49:201–3.

98. Trefts E, Gannon M, Wasserman DH. The liver. Curr Biol 2017;27:R1147–51.

99. Tsung A, Geller DA. Gross and Cellular Anatomy of the Liver. In book: Monga PS, edit. Molecular Pathology of Liver Diseases. Springer Boston, MA US; 2011:3-6

100. Stanger BZ. Cellular homeostasis and repair in the mammalian liver. Annu Rev Physiol 2015;77:179–200.

101. Uhlén M, Fagerberg L, Hallström BM, et al. Tissue-based map of the human proteome. Science 2015;347:6220.

102. Watt MJ, Miotto PM, De Nardo W, Montgomery MK. The liver as an endocrine organ—linking NAFLD and insulin resistance. Endocr Rev 2019;40:1367–93.

103. Fellman V, Kotarsky H. Mitochondrial hepatopathies in the newborn period. Semin Fetal Neonatal Med 2011;16:222–8.

104. Mandel H, Hartman C, Berkowitz D, Elpeleg ON, Manov I, Iancu TC. The hepatic mitochondrial DNA depletion syndrome: ultrastructural changes in liver biopsies. Hepatology 2001;34:776–84.

105. Pronicka E, Węglewska-Jurkiewicz A, Taybert J, et al. Post mortem identification of deoxyguanosine kinase (DGUOK) gene mutations combined with impaired glucose homeostasis and iron overload features in four infants with severe progressive liver failure. J Appl Genet 2011;52:61–6.

106. Valnot I, Osmond S, Gigarel N, et al. Mutations of the SCO1 gene in mitochondrial cytochrome c oxidase deficiency with neonatal-onset hepatic failure and encephalopathy. Am J Hum Genet 2000;67:1104–9.

107. Lee J, Choi J, Scafidi S, Wolfgang MJ. Hepatic fatty acid oxidation restrains systemic catabolism during starvation. Cell Rep 2016;16:201–12.

108. Perry RJ, Kim T, Zhang X-M, et al. Reversal of Hypertriglyceridemia, Fatty Liver Disease, and Insulin Resistance by a Liver-Targeted Mitochondrial Uncoupler. Cell

Metab 2013;18:740–8.

109. Cho J, Zhang Y, Park S-Y, et al. Mitochondrial ATP transporter depletion protects mice against liver steatosis and insulin resistance. Nat Commun 2017;8:14477.

110. Tormos KV, Anso E, Hamanaka RB, et al. Mitochondrial complex III ROS regulate adipocyte differentiation. Cell Metab 2011;14:537–44.

111. Diebold LP, Gil HJ, Gao P, Martinez CA, Weinberg SE, Chandel NS. Mitochondrial complex III is necessary for endothelial cell proliferation during angiogenesis. Nat Metab 2019;1:158–71.

112. Waypa GB, Marks JD, Guzy RD, et al. Superoxide generated at mitochondrial complex III triggers acute responses to hypoxia in the pulmonary circulation. Am J Respir Crit Care Med 2013;187:424–32.

113. Sena LA, Li S, Jairaman A, et al. Mitochondria are required for antigen-specific T cell activation through reactive oxygen species signaling. Immunity 2013;38:225–36.

114. Hughes BG, Hekimi S. A mild impairment of mitochondrial electron transport has sex-specific effects on lifespan and aging in mice. PLOS ONE 2011;6:e26116.

115. Spinazzi M, Radaelli E, Horré K, et al. PARL deficiency in mouse causes Complex III defects, coenzyme Q depletion, and Leigh-like syndrome. Proc Natl Acad Sci 2019;116:277–86.

116. Davoudi M, Kotarsky H, Hansson E, Kallijärvi J, Fellman V. COX7A2L/SCAFI and pre-complex III modify respiratory chain supercomplex formation in different mouse strains with a Bcs1l Mutation. PLOS ONE 2016;11:e0168774.

117. Rajendran J, Tomašić N, Kotarsky H, et al. Effect of high-carbohydrate diet on plasma metabolome in mice with mitochondrial respiratory chain complex III deficiency. Int J Mol Sci 2016;17:1824.

118. Russell OM, Gorman GS, Lightowlers RN, Turnbull DM. Mitochondrial diseases: Hope for the future. Cell 2020;181:168–88.

119. Viscomi C, Zeviani M. Strategies for fighting mitochondrial diseases. J Intern Med 287:665–84.

120. Domínguez-González C, Madruga-Garrido M, Mavillard F, et al. Deoxynucleoside therapy for thymidine kinase 2–deficient myopathy. Ann Neurol 2019;86:293–303.

121. Diaz F, Garcia S, Hernandez D, et al. Pathophysiology and fate of hepatocytes in a mouse model of mitochondrial hepatopathies. Gut 2008;57:232–42.

122. Rossmanith W, Freilinger M, Roka J, et al. Isolated cytochrome c oxidase deficiency

as a cause of MELAS. J Med Genet 2008;45:117–21.

123. Black JT, Judge D, Demers L, Gordon S. Ragged-red fibers: A biochemical and morphological study. J Neurol Sci 1975;26:479–88.

124. Cantó C, Auwerx J. PGC-1alpha, SIRT1 and AMPK, an energy sensing network that controls energy expenditure. Curr Opin Lipidol 2009;20:98–105.

125. Viscomi C, Bottani E, Civiletto G, et al. In vivo correction of COX deficiency by activation of the AMPK/PGC-1α axis. Cell Metab 2011;14:80–90.

126. Martínez-Redondo V, Pettersson AT, Ruas JL. The hitchhiker's guide to PGC-1α isoform structure and biological functions. Diabetologia 2015;58:1969–77.

127. Peralta S, Garcia S, Yin HY, Arguello T, Diaz F, Moraes CT. Sustained AMPK activation improves muscle function in a mitochondrial myopathy mouse model by promoting muscle fiber regeneration. Hum Mol Genet 2016;25:3178–91.

128. Katsyuba E, Romani M, Hofer D, Auwerx J. NAD+ homeostasis in health and disease. Nat Metab 2020;2:9–31.

129. Cantó C, Houtkooper RH, Pirinen E, et al. The NAD+ precursor nicotinamide riboside enhances oxidative metabolism and protects against high-fat diet-induced obesity. Cell Metab 2012;15:838–47.

130. Cerutti R, Pirinen E, Lamperti C, et al. NAD+-dependent activation of Sirt1 corrects the phenotype in a mouse model of mitochondrial disease. Cell Metab 2014;19:1042–9.

131. Khan NA, Auranen M, Paetau I, et al. Effective treatment of mitochondrial myopathy by nicotinamide riboside, a vitamin B3. EMBO Mol Med 2014;6:721–31.

132. Hondares E, Mora O, Yubero P, et al. Thiazolidinediones and rexinoids induce peroxisome proliferator-activated receptor-coactivator (PGC)-1α gene transcription: An autoregulatory loop controls PGC-1α expression in adipocytes via peroxisome proliferator-activated receptor-γ coactivation. Endocrinology 2006;147:2829–38.

133. Schuler M, Ali F, Chambon C, et al. PGC1α expression is controlled in skeletal muscles by PPARβ, whose ablation results in fiber-type switching, obesity, and type 2 diabetes. Cell Metab 2006;4:407–14.

134. Bastin J, Aubey F, Rötig A, Munnich A, Djouadi F. Activation of peroxisome proliferator-activated receptor pathway stimulates the mitochondrial respiratory chain and can correct deficiencies in patients' cells lacking its components. J Clin Endocrinol Metab 2008;93:1433–41.

135. Yatsuga S, Suomalainen A. Effect of bezafibrate treatment on late-onset mitochondrial myopathy in mice. Hum Mol Genet 2012;21:526–35.

136. Dillon LM, Williams SL, Hida A, et al. Increased mitochondrial biogenesis in muscle improves aging phenotypes in the mtDNA mutator mouse. Hum Mol Genet 2012;21:2288–97.

137. Steele H, Gomez-Duran A, Pyle A, et al. Metabolic effects of bezafibrate in mitochondrial disease. EMBO Mol Med 2020;12:e11589.

138. Jewell JL, Guan K-L. Nutrient signaling to mTOR and cell growth. Trends Biochem Sci 2013;38:233–42.

139. Johnson SC, Yanos M, Sangesland M, et al. Dose-dependent effects of mTOR inhibition on weight and mitochondrial disease in mice. Front Genet 2015;6:247.

140. Siegmund SE, Yang H, Sharma R, et al. Low-dose rapamycin extends lifespan in a mouse model of mtDNA depletion syndrome. Hum Mol Genet 2017;26:4588–605.

141. Civiletto G, Dogan SA, Cerutti R, et al. Rapamycin rescues mitochondrial myopathy via coordinated activation of autophagy and lysosomal biogenesis. EMBO Mol Med 2018;10:e8799.

142. Khan NA, Nikkanen J, Yatsuga S, et al. mTORC1 regulates mitochondrial integrated stress response and mitochondrial myopathy progression. Cell Metab 2017;26:419-428.e5.

143. Barriocanal-Casado E, Hidalgo-Gutiérrez A, Raimundo N, et al. Rapamycin administration is not a valid therapeutic strategy for every case of mitochondrial disease. EBioMedicine 2019;42:511–23.

144. Branco AF, Ferreira A, Simões RF, et al. Ketogenic diets: from cancer to mitochondrial diseases and beyond. Eur J Clin Invest 2016;46:285–98.

145. Nyenwe EA, Kitabchi AE. The evolution of diabetic ketoacidosis: An update of its etiology, pathogenesis and management. Metabolism 2016;65:507–21.

146. Owen OE, Morgan AP, Kemp HG, Sullivan JM, Herrera MG, Cahill GF. Brain metabolism during fasting. J Clin Invest 1967;46:1589–95.

147. Owen OE, Felig P, Morgan AP, Wahren J, Cahill GF. Liver and kidney metabolism during prolonged starvation. J Clin Invest 1969;48:574–83.

148. Liu YC. Medium-chain triglyceride (MCT) ketogenic therapy. Epilepsia 2008;49:33–6.

149. Bielohuby M, Menhofer D, Kirchner H, et al. Induction of ketosis in rats fed low-carbohydrate, high-fat diets depends on the relative abundance of dietary fat and protein. Am J Physiol - Endocrinol Metab 2011;300:E65–76.

150. Schugar RC, Huang X, Moll AR, Brunt EM, Crawford PA. Role of choline deficiency

in the fatty liver phenotype of mice fed a low protein, very low carbohydrate ketogenic diet. PLOS ONE 2013;8:e74806.

151. Pissios P, Hong S, Kennedy AR, Prasad D, Liu F-F, Maratos-Flier E. Methionine and choline regulate the metabolic phenotype of a ketogenic diet. Mol Metab 2013;2:306–13.

152. Badman MK, Pissios P, Kennedy AR, Koukos G, Flier JS, Maratos-Flier E. Hepatic fibroblast growth factor 21 Is regulated by PPARα and is a key mediator of hepatic lipid metabolism in ketotic states. Cell Metab 2007;5:426–37.

153. BonDurant LD, Potthoff MJ. Fibroblast growth factor 21: A versatile regulator of metabolic homeostasis. Annu Rev Nutr 2018;38:173–96.

154. McGree CD, Lieberman P, Greenwood CE. Dietary fatty acid composition induces comparable changes in cardiolipin fatty acid profile of heart and brain mitochondria. Lipids 1996;31:611–6.

155. Mulligan CM, Sparagna GC, Le CH, et al. Dietary linoleate preserves cardiolipin and attenuates mitochondrial dysfunction in the failing rat heart. Cardiovasc Res 2012;94:460–8.

156. Wahli W, Michalik L. PPARs at the crossroads of lipid signaling and inflammation. Trends Endocrinol Metab 2012;23:351–63.

157. Hock MB, Kralli A. Transcriptional control of mitochondrial biogenesis and function. Annu Rev Physiol 2009;71:177–203.

158. Tomašić N, Kotarsky H, de Oliveira Figueiredo R, et al. Fasting reveals largely intact systemic lipid mobilization mechanisms in respiratory chain complex III deficient mice. Biochim Biophys Acta Mol Basis Dis 2020;1866:165573.

159. Miller KN, Clark JP, Martin SA, et al. PGC-1a integrates a metabolism and growth network linked to caloric restriction. Aging Cell 2019;18:e12999.

160. Lanza IR, Zabielski P, Klaus KA, et al. Chronic caloric restriction preserves mitochondrial function in senescence without increasing mitochondrial biogenesis. Cell Metab 2012;16:777–88.

161. Wheless JW. History of the ketogenic diet. Epilepsia 2008;49:3–5.

162. Bough KJ, Wetherington J, Hassel B, et al. Mitochondrial biogenesis in the anticonvulsant mechanism of the ketogenic diet. Ann Neurol 2006;60:223–35.

163. Peralta S, Torraco A, Iommarini L, Diaz F. Mitochondrial diseases part III: Therapeutic interventions in mouse models of OXPHOS deficiencies. Mitochondrion 2015;23:71–80.

164. Santra S, Gilkerson RW, Davidson M, Schon EA. Ketogenic treatment reduces deleted mitochondrial DNAs in cultured human cells. Ann Neurol 2004;56:662–9.

165. Emperador S, López-Gallardo E, Hernández-Ainsa C, et al. Ketogenic treatment reduces the percentage of a LHON heteroplasmic mutation and increases mtDNA amount of a LHON homoplasmic mutation. Orphanet J Rare Dis 2019;14:150.

166. Frey S, Geffroy G, Desquiret-Dumas V, et al. The addition of ketone bodies alleviates mitochondrial dysfunction by restoring complex I assembly in a MELAS cellular model. Biochim Biophys Acta BBA - Mol Basis Dis 2017;1863:284–91.

167. Ahola-Erkkilä S, Carroll C, Peltola-Mjösund K, et al. Ketogenic diet slows down mitochondrial myopathy progression in mice. Hum Mol Genet 2010;19:1974-84.

168. Tischner C, Hofer A, Wulff V, et al. MTO1 mediates tissue specificity of OXPHOS defects via tRNA modification and translation optimization, which can be bypassed by dietary intervention. Hum Mol Genet 2015;24:2247–66.

169. Martin-McGill KJ, Jackson CF, Bresnahan R, Levy RG, Cooper PN. Ketogenic diets for drug-resistant epilepsy. Cochrane Database Syst Rev 2018;11:CD001903.

170. Sofou K, Dahlin M, Hallböök T, Lindefeldt M, Viggedal G, Darin N. Ketogenic diet in pyruvate dehydrogenase complex deficiency: short- and long-term outcomes. J Inherit Metab Dis 2017;40:237–45.

171. Schwantje M, Verhagen LM, van Hasselt PM, Fuchs SA. Glucose transporter type 1 deficiency syndrome and the ketogenic diet. J Inherit Metab Dis 2020;43:216–22.

172. Kang H-C, Lee Y-M, Kim HD, Lee JS, Slama A. Safe and effective use of the ketogenic diet in children with epilepsy and mitochondrial respiratory chain complex defects. Epilepsia 2007;48:82–8.

173. Ahola S, Auranen M, Isohanni P, et al. Modified Atkins diet induces subacute selective ragged-red-fiber lysis in mitochondrial myopathy patients. EMBO Mol Med 2016;8:1234–47.

174. Marina AD, Leiendecker B, Roesch S, Wortmann SB. Ketogenic diet for treating alopecia in BCS1l-related mitochondrial disease (Bjornstad syndrome). JIMD Rep 53:10–1.

175. Youm Y-H, Nguyen KY, Grant RW, et al. The ketone metabolite β-hydroxybutyrate blocks NLRP3 inflammasome-mediated inflammatory disease. Nat Med 2015;21:263–9.

176. Taggart AKP, Kero J, Gan X, et al. (d)-β-Hydroxybutyrate inhibits adipocyte lipolysis via the nicotinic acid receptor PUMA-G. J Biol Chem 2005;280:26649–52.

177. Shimazu T, Hirschey MD, Newman J, et al. Suppression of oxidative stress by β-hydroxybutyrate, an endogenous histone deacetylase inhibitor. Science 2013;339:211–4.

178. Chriett S, Dąbek A, Wojtala M, Vidal H, Balcerczyk A, Pirola L. Prominent action of butyrate over β-hydroxybutyrate as histone deacetylase inhibitor, transcriptional modulator and anti-inflammatory molecule. Sci Rep 2019;9:1–14.

179. Chalkiadaki A, Guarente L. The multifaceted functions of sirtuins in cancer. Nat Rev Cancer 2015;15:608–24.

180. Hurtado-Bagès S, Knobloch G, Ladurner AG, Buschbeck M. The taming of PARP1 and its impact on NAD+ metabolism. Mol Metab 2020;38:100950.

181. Camacho-Pereira J, Tarragó MG, Chini CCS, et al. CD38 dictates age-related NAD decline and mitochondrial dysfunction through an SIRT3-dependent mechanism. Cell Metab 2016;23:1127–39.

182. Liu H, Smith CB, Schmidt MS, et al. Pharmacological bypass of NAD+ salvage pathway protects neurons from chemotherapy-induced degeneration. Proc Natl Acad Sci 2018;115:10654–9.

183. Rodgers JT, Lerin C, Haas W, Gygi SP, Spiegelman BM, Puigserver P. Nutrient control of glucose homeostasis through a complex of PGC-1α and SIRT1. Nature 2005;434:113–8.

184. Wagner GR, Payne RM. Widespread and enzyme-independent Nε-acetylation and Nε-succinylation of proteins in the chemical conditions of the mitochondrial matrix. J Biol Chem 2013;288:29036–45.

185. James AM, Hoogewijs K, Logan A, et al. Non-enzymatic N-acetylation of lysine residues by acetylCoA often occurs via a proximal S-acetylated thiol intermediate sensitive to glyoxalase II. Cell Rep 2017;18:2105–12.

186. Hasmann M, Schemainda I. FK866, a highly specific noncompetitive inhibitor of nicotinamide phosphoribosyltransferase, represents a novel mechanism for induction of tumor cell apoptosis. Cancer Res 2003;63:7436–42.

187. Revollo JR, Grimm AA, Imai S. The NAD biosynthesis pathway mediated by nicotinamide phosphoribosyltransferase regulates Sir2 activity in mammalian cells. J Biol Chem 2004;279:50754–63.

188. Ramsey KM, Yoshino J, Brace CS, et al. Circadian clock feedback cycle through NAMPT-mediated NAD+ biosynthesis. Science 2009;324:651–4.

189. Nakahata Y, Sahar S, Astarita G, Kaluzova M, Sassone-Corsi P. Circadian control of the NAD+ salvage pathway by CLOCK-SIRT1. Science 2009;324:654–7.

190. Shats I, Williams JG, Liu J, et al. Bacteria boost mammalian host NAD metabolism by engaging the deamidated biosynthesis pathway. Cell Metab 2020;31:564-579.e7.

191. Collins PB, Chaykin S. The management of nicotinamide and nicotinic acid in the mouse. J Biol Chem 1972;247:778–83.

192. Liu L, Su X, Quinn WJ, et al. Quantitative analysis of NAD synthesis-breakdown fluxes. Cell Metab 2018;27:1067-1080.e5.

193. Bieganowski P, Brenner C. Discoveries of nicotinamide riboside as a nutrient and conserved NRK genes establish a Preiss-Handler independent route to NAD+ in fungi and humans. Cell 2004;117:495–502.

194. Benyó Z, Gille A, Kero J, et al. GPR109A (PUMA-G/HM74A) mediates nicotinic acid–induced flushing. J Clin Invest 2005;115:3634–40.

195. Gardell SJ, Hopf M, Khan A, et al. Boosting NAD + with a small molecule that activates NAMPT. Nat Commun 2019;10:1–12.

196. Avalos JL, Bever KM, Wolberger C. Mechanism of sirtuin inhibition by nicotinamide: Altering the NAD+ cosubstrate specificity of a Sir2 enzyme. Mol Cell 2005;17:855–68.

197. Giroud-Gerbetant J, Joffraud M, Giner MP, et al. A reduced form of nicotinamide riboside defines a new path for NAD+ biosynthesis and acts as an orally bioavailable NAD+ precursor. Mol Metab 2019;30:192–202.

198. Yang Y, Mohammed FS, Zhang N, Sauve AA. Dihydronicotinamide riboside is a potent NAD+ concentration enhancer in vitro and in vivo. J Biol Chem 2019;294:9295–307.

199. Yang Y, Zhang N, Zhang G, Sauve AA. NRH salvage and conversion to NAD + requires NRH kinase activity by adenosine kinase. Nat Metab 2020;2:364–79.

200. Hegyi J, Schwartz RA, Hegyi V. Pellagra: Dermatitis, dementia, and diarrhea. Int J Dermatol 2004;43:1–5.

201. Gariani K, Menzies KJ, Ryu D, et al. Eliciting the mitochondrial unfolded protein response by nicotinamide adenine dinucleotide repletion reverses fatty liver disease in mice. Hepatology 2016;63:1190–204.

202. Trammell SAJ, Weidemann BJ, Chadda A, et al. Nicotinamide Riboside Opposes Type 2 Diabetes and Neuropathy in Mice. Sci Rep 2016;6:26933.

203. Ryu D, Zhang H, Ropelle ER, et al. NAD+ repletion improves muscle function in muscular dystrophy and counters global PARylation. Sci Transl Med 2016;8:361ra139

204. Diguet Nicolas, Trammell Samuel A.J., Tannous Cynthia, et al. Nicotinamide riboside preserves cardiac function in a mouse model of dilated cardiomyopathy. Circulation

2018;137(21):2256–73.

205. Katsyuba E, Mottis A, Zietak M, et al. De novo NAD + synthesis enhances mitochondrial function and improves health. Nature 2018;563:354–9.

206. Lee CF, Caudal A, Abell L, Gowda GAN, Tian R. Targeting NAD+ metabolism as interventions for mitochondrial fisease. Sci Rep 2019;9:1–10.

207. Mills KF, Yoshida S, Stein LR, et al. Long-term administration of nicotinamide mononucleotide mitigates age-associated physiological decline in mice. Cell Metab 2016;24:795–806.

208. Pirinen E, Cantó C, Jo YS, et al. Pharmacological inhibition of poly(ADP-ribose) polymerases improves fitness and mitochondrial function in skeletal muscle. Cell Metab 2014;19:1034–41.

209. Dollerup OL, Chubanava S, Agerholm M, et al. Nicotinamide riboside does not alter mitochondrial respiration, content or morphology in skeletal muscle from obese and insulin-resistant men. J Physiol 2020;598:731–54.

210. Elhassan YS, Kluckova K, Fletcher RS, et al. Nicotinamide riboside augments the aged human skeletal muscle NAD+ metabolome and induces transcriptomic and anti-inflammatory signatures. Cell Rep 2019;28:1717-1728.e6.

211. Pirinen E, Auranen M, Khan NA, et al. Niacin cures systemic NAD+ deficiency and improves muscle performance in adult-onset mitochondrial myopathy. Cell Metab 2020;31:1078-1090.e5.

212. McDonald AE, Gospodaryov DV. Alternative NAD(P)H dehydrogenase and alternative oxidase: Proposed physiological roles in animals. Mitochondrion 2019;45:7–17.

213. Wagner null, Wagner null, Moore null. In vivo ubiquinone reduction levels during thermogenesis in araceae. Plant Physiol 1998;117:1501–6.

214. Chaudhuri M, Ott RD, Hill GC. Trypanosome alternative oxidase: from molecule to function. Trends Parasitol 2006;22:484–91.

215. Hakkaart GAJ, Dassa EP, Jacobs HT, Rustin P. Allotopic expression of a mitochondrial alternative oxidase confers cyanide resistance to human cell respiration. EMBO Rep 2006;7:341–5.

216. Guarás A, Perales-Clemente E, Calvo E, et al. The CoQH2/CoQ ratio serves as a sensor of respiratory chain efficiency. Cell Rep 2016;15:197–209.

217. Protasoni M, Pérez-Pérez R, Lobo-Jarne T, et al. Respiratory supercomplexes act as a platform for complex III-mediated maturation of human mitochondrial complexes I and IV. EMBO J 2020;39:e102817.

218. El-Khoury R, Dufour E, Rak M, et al. Alternative oxidase expression in the mouse enables bypassing cytochrome c oxidase blockade and limits mitochondrial ROS overproduction. PLOS Genet 2013;9:e1003182.

219. Szibor M, Dhandapani PK, Dufour E, et al. Broad AOX expression in a genetically tractable mouse model does not disturb normal physiology. Dis Model Mech 2017;10:163–71.

220. Bajzikova M, Kovarova J, Coelho AR, et al. Reactivation of dihydroorotate dehydrogenase-driven pyrimidine biosynthesis restores tumor growth of respiration-deficient cancer cells. Cell Metab 2019;29:399-416.e10.

221. Sommer N, Alebrahimdehkordi N, Pak O, et al. Bypassing mitochondrial complex III using alternative oxidase inhibits acute pulmonary oxygen sensing. Sci Adv 2020;6:eaba0694.

222. Mills EL, O'Neill LA. Reprogramming mitochondrial metabolism in macrophages as an anti-inflammatory signal. Eur J Immunol 2016;46:13–21.

223. Kotarsky H, Keller M, Davoudi M, et al. Metabolite profiles reveal energy failure and impaired beta-oxidation in liver of mice with complex III deficiency due to a BCS1L mutation. PLOS ONE 2012;7:e41156.

224. Van Haele M, Roskams T. Hepatic progenitor cells: An update. Gastroenterol Clin North Am 2017;46:409–20.

225. Eleazar JA, Memeo L, Jhang JS, et al. Progenitor cell expansion: an important source of hepatocyte regeneration in chronic hepatitis. J Hepatol 2004;41:983–91.

226. Español–Suñer R, Carpentier R, Van Hul N, et al. Liver progenitor cells yield functional hepatocytes in response to chronic liver injury in mice. Gastroenterology 2012;143:1564-1575.e7.

227. Lu W-Y, Bird TG, Boulter L, et al. Hepatic progenitor cells of biliary origin with liver repopulation capacity. Nat Cell Biol 2015;17:971–83.

228. Cogliati S, Frezza C, Soriano ME, et al. Mitochondrial cristae shape determines respiratory chain supercomplexes assembly and respiratory efficiency. Cell 2013;155:160–71.

229. Patten DA, Wong J, Khacho M, et al. OPA1-dependent cristae modulation is essential for cellular adaptation to metabolic demand. EMBO J 2014;33:2676–91.

230. Gomes LC, Benedetto GD, Scorrano L. During autophagy mitochondria elongate, are spared from degradation and sustain cell viability. Nat Cell Biol 2011;13:589–98.

231. Jin Z, Wei W, Yang M, Du Y, Wan Y. Mitochondrial complex I activity suppresses

inflammation and enhances bone resorption by shifting macrophage-osteoclast polarization. Cell Metab 2014;20:483–98.

232. Weinberg SE, Singer BD, Steinert EM, et al. Mitochondrial complex III is essential for suppressive function of regulatory T cells. Nature 2019;565:495–9.

233. Chen Y, Ouyang X, Hoque R, et al. B-hydroxybutyrate protects from alcohol-induced liver injury via a Hcar2-cAMP dependent pathway. J Hepatol 2018;69:687–96.

234. Trammell SAJ, Schmidt MS, Weidemann BJ, et al. Nicotinamide riboside is uniquely and orally bioavailable in mice and humans. Nat Commun 2016;7:12948.

235. Zhang C-S, Hawley SA, Zong Y, et al. Fructose-1,6-bisphosphate and aldolase mediate glucose sensing by AMPK. Nature 2017;548:112–6.

236. Gerhart-Hines Z, Dominy JE, Blättler SM, et al. The cAMP/PKA pathway rapidly activates SIRT1 to promote fatty acid oxidation independently of changes in NAD(+). Mol Cell 2011;44:851–63.

237. Wang Z, Zhang L, Liang Y, et al. Cyclic AMP mimics the anti-ageing effects of calorie restriction by up-regulating sirtuin. Sci Rep 2015;5:12012.

238. Fulco M, Cen Y, Zhao P, et al. Glucose restriction inhibits skeletal myoblast differentiation by activating SIRT1 through AMPK-mediated regulation of Nampt. Dev Cell 2008;14:661–73.

239. Gariani K, Ryu D, Menzies KJ, et al. Inhibiting poly ADP-ribosylation increases fatty acid oxidation and protects against fatty liver disease. J Hepatol 2017;66:132–41.

240. Wellen KE, Hatzivassiliou G, Sachdeva UM, Bui TV, Cross JR, Thompson CB. ATP-citrate lyase links cellular metabolism to histone acetylation. Science 2009;324:1076–80.

241. Rajendran J. Interventions to improve mitochondrial function in a mouse model of GRACILE syndrome, a complex III disorder. Thesis, University of Helsinki 2019, available:http://urn.fi/URN:ISBN:978-951-51-4948-0

242. Lehtonen JM, Forsström S, Bottani E, et al. FGF21 is a biomarker for mitochondrial translation and mtDNA maintenance disorders. Neurology 2016;87:2290–9.

243. Ostojić J, Panozzo C, Lasserre J-P, et al. The energetic state of mitochondria modulates complex III biogenesis through the ATP-dependent activity of Bcs1. Cell Metab 2013;18:567–77.

244. Dogan SA, Cerutti R, Benincá C, et al. Perturbed redox signaling exacerbates a mitochondrial myopathy. Cell Metab 2018;28:764–75.

245. Borek A, Kuleta P, Ekiert R, Pietras R, Sarewicz M, Osyczka A. Mitochondrial disease-related mutation G167P in cytochrome b of rhodobacter capsulatus cytochrome bc1 (S151P in human) affects the equilibrium distribution of [2Fe-2S] cluster and generation of superoxide. J Biol Chem 2015;290:23781–92.

246. Castellani M, Covian R, Kleinschroth T, Anderka O, Ludwig B, Trumpower BL. Direct demonstration of half-of-the-sites reactivity in the dimeric cytochrome bc1 complex enzyme with one inactive monomer is fully active but unable to activate the second ubiquinol oxidation site in response to ligand binding at the ubiquinone reduction site. J Biol Chem 2010;285:502–10.

247. Świerczek M, Cieluch E, Sarewicz M, et al. An electronic bus bar lies in the core of cytochrome bc1. Science 2010;329:451–4.

248. Schmitt ME, Trumpower BL. Subunit 6 regulates half-of-the-sites reactivity of the dimeric cytochrome bc1 complex in Saccharomyces cerevisiae. J Biol Chem 1990;265:17005–11.

249. Forsström S, Jackson CB, Carroll CJ, et al. Fibroblast growth factor 21 drives dynamics of local and systemic stress responses in mitochondrial myopathy with mtDNA deletions. Cell Metab 2019;30:1040–54.

250. Newman JC, Verdin E. Ketone bodies as signaling metabolites. Trends Endocrinol Metab 2014;25:42–52.

251. Liu K, Li F, Sun Q, et al. p53 β-hydroxybutyrylation attenuates p53 activity. Cell Death Dis 2019;10:1–13.

252. Clarke K, Tchabanenko K, Pawlosky R, et al. Kinetics, safety and tolerability of (R)-3-hydroxybutyl (R)-3-hydroxybutyrate in healthy adult subjects. Regul Toxicol Pharmacol 2012;63:401–8.

253. McDonald AE, Vanlerberghe GC, Staples JF. Alternative oxidase in animals: unique characteristics and taxonomic distribution. J Exp Biol 2009;212:2627–34.

254. Cliffe RN, Haupt RJ, Avey-Arroyo JA, Wilson RP. Sloths like it hot: ambient temperature modulates food intake in the brown-throated sloth (Bradypus variegatus). PeerJ 2015;3:e875.